

## Spectroscopic Study of Electron Transfer in a Trifunctional Lysine with Anthraquinone as the Electron Acceptor

Sandra L. Mecklenburg, Dewey G. McCafferty, Jon R. Schoonover, Brian M. Peek, Bruce W. Erickson,\* and Thomas J. Meyer\*

Department of Chemistry, University of North Carolina, Chapel Hill, North Carolina 27599-3290

Received October 29, 1993\*

The transient properties of the redox-active amino acid dyads [Anq-Lys(Ru<sup>II</sup>b<sub>2</sub>m)<sup>2+</sup>-OCH<sub>3</sub>](PF<sub>6</sub>)<sub>2</sub> and [Boc-Lys(Ru<sup>II</sup>b<sub>2</sub>m)<sup>2+</sup>-NH-prPTZ](PF<sub>6</sub>)<sub>2</sub> and the trifunctionalized amino acid [Anq-Lys(Ru<sup>II</sup>b<sub>2</sub>m)<sup>2+</sup>-NH-prPTZ](PF<sub>6</sub>)<sub>2</sub>, where Anq is 9,10-anthraquinone-2-carbonyl, Lys is L-lysine, b is 2,2'-bipyridine, m is 4'-methyl-2,2'-bipyridine-4-carbonyl, and prPTZ is 3-(10*H*-phenothiazine-10)propyl, were examined in CH<sub>3</sub>CN after nanosecond laser excitation. This series of redox-active assemblies was prepared by attaching derivatives of the ruthenium tris(bipyridyl) chromophore, the electron donor phenothiazine, and/or the electron acceptor anthraquinone to L-lysine with amide bonds. Emission from the chromophore was efficiently quenched (>95%) by the attached donors or acceptors in all three cases. Irradiation of [Anq-Lys(Ru<sup>II</sup>b<sub>2</sub>m)<sup>2+</sup>-NH-prPTZ] with 420-nm, 4-ns laser pulses resulted in net electron transfer from prPTZ to Anq, mediated by the metal-to-ligand charge-transfer (MLCT) excited state of the ruthenium chromophore, as observed by nanosecond transient absorption and time-resolved resonance Raman spectroscopies. The resulting redox-separated state, [(Anq<sup>-</sup>)-Lys(Ru<sup>II</sup>b<sub>2</sub>m)<sup>2+</sup>-NH-(prPTZ<sup>•+</sup>)], at 1.54 eV, was formed with a quantum efficiency of 26% at its maximum appearance and persisted for 174 ns in CH<sub>3</sub>CN at 25 °C.

### Introduction

Intramolecular photoinduced redox separation in molecules containing both an electron-transfer donor and an acceptor as well as a chromophore has previously been achieved in carotenoid porphyrin-quinones,<sup>1</sup> aniline porphyrin-quinones,<sup>2</sup> and ruthenium polypyridyl complexes.<sup>3,4</sup> The secondary structures of peptides have been exploited to provide controlled orientation or spacing of photoactive sites in studies of intramolecular electron transfer.<sup>5-7</sup> By combining these two concepts, we report here a second example of a redox-active assembly in which a single amino acid has been

functionalized with an electron-transfer donor, a chromophore, and an electron-transfer acceptor. The redox-active modules are attached to lysine through amide bonds. Previously we reported the photophysical properties of the lysine-based triad [PTZpn-Lys(Ru<sup>II</sup>b<sub>2</sub>m)<sup>2+</sup>-NH-prPQ<sup>2+</sup>](PF<sub>6</sub>)<sub>2</sub> (Chart 1).<sup>4,8</sup> Here we describe the preparation and photophysical behavior of the triad [Anq-Lys(Ru<sup>II</sup>b<sub>2</sub>m)<sup>2+</sup>-NH-prPTZ](PF<sub>6</sub>)<sub>2</sub>, which utilizes the electron acceptor anthraquinone in place of paraquat. Upon irradiation, these assemblies undergo a series of electron-transfer events that lead to redox separation.

### Experimental Section

**Materials.** The following compounds were prepared and purified as described previously:<sup>9</sup> 4'-methyl-2,2'-bipyridine-4-carboxylic acid, (m-OH); bis(2,2'-bipyridine)(4'-methyl-2,2'-bipyridine-4-carboxamidomethane)ruthenium(II) bis(hexafluorophosphate), [(Ru<sup>II</sup>b<sub>2</sub>m-NHCH<sub>3</sub>)<sup>2+</sup>](PF<sub>6</sub>)<sub>2</sub>; *N*<sup>α</sup>-(1,1-dimethylethoxycarbonyl)-*N*<sup>ε</sup>-(bis(2,2'-bipyridine)(4'-methyl-2,2'-bipyridine-4-carbonyl)ruthenium(II))-L-lysine bis(hexafluorophosphate), [Boc-Lys(Ru<sup>II</sup>b<sub>2</sub>m)<sup>2+</sup>-OH](PF<sub>6</sub>)<sub>2</sub>; *N*<sup>α</sup>-(1,1-dimethylethoxycarbonyl)-*N*<sup>ε</sup>-(bis(2,2'-bipyridine)(4'-methyl-2,2'-bipyridine-4-carbonyl)ruthenium(II))-L-lysine methyl ester bis(hexafluorophosphate), [Boc-Lys(Ru<sup>II</sup>b<sub>2</sub>m)<sup>2+</sup>-OCH<sub>3</sub>](PF<sub>6</sub>)<sub>2</sub>; 3-(10*H*-phenothiazine-10)propylamine hydrochloride, PTZpr-NH<sub>2</sub>·HCl.<sup>4b,10</sup>

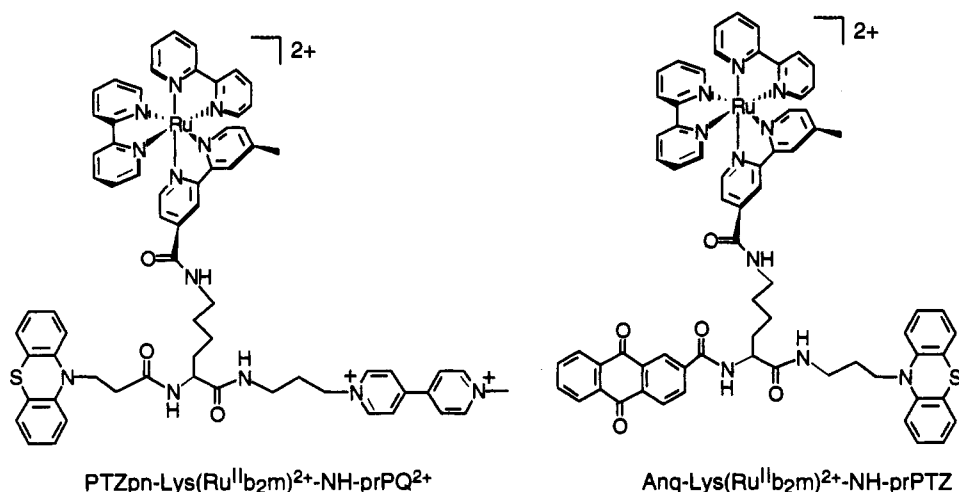
**General Methods.** Uncorrected melting points and the UV-visible, infrared, mass, and <sup>1</sup>H NMR spectra were recorded as described previously.<sup>4b</sup> Cation-exchange HPLC was performed with an Aquapore CX-300 column (1.0 cm × 10 cm) of poly(DL-Asp)-silica (Brownlee) with a gradient of 0–400 mM KBr in 2:3 (v/v) CH<sub>3</sub>CN/0.6 mM phosphate buffer (pH 7.2).

\* Abstract published in *Advance ACS Abstracts*, May 15, 1994.

- (1) (a) Gust, D.; Moore, T. A.; Moore, A. L.; et al. *J. Am. Chem. Soc.* **1991**, *113*, 3638. (b) Gust, D.; Moore, T. A.; Moore, A. L.; Lee, S.-J.; Bittersmann, E.; Luttrull, D. K.; Rehms, A. A.; DeGraziano, J. M.; Ma, X. C.; Gao, F.; Belford, R. E.; Trier, T. T. *Science* **1990**, *248*, 199. (c) Gust, D.; Moore, T. A. *Science* **1989**, *244*, 35. (d) Gust, D.; Moore, T. A.; Moore, A. L.; Makings, L. R.; Seely, G. R.; Ma, X.; Trier, T. T.; Gao, F. *J. Am. Chem. Soc.* **1988**, *110*, 7567. (e) Moore, T. A.; Gust, D.; Mathis, P.; Mialocq, J.-C.; Chachaty, C.; Bensusson, R. V.; Band, E. J.; Doizi, D.; Liddell, P. A.; Lehman, W. R.; Nemeth, G. A.; Moore, A. L. *Nature* **1984**, *307*, 630.
- (2) (a) Wasielewski, M. R.; Gaines, G. L., III.; O'Neil, M. P.; Svec, W. A.; Niemczyk, M. P. *J. Am. Chem. Soc.* **1990**, *112*, 4559. (b) Hofstra, U.; Schaafsma, T. J.; Sanders, G. M.; Van Dijk, M.; Van Der Plas, H. C.; Johnson, D. G.; Wasielewski, M. R. *Chem. Phys. Lett.* **1988**, *151*, 169. (c) Schmidt, J. A.; McIntosh, A. R.; Weedon, A. C.; Bolton, J. R.; Connolly, J. S.; Hurley, J. K.; Wasielewski, M. R. *J. Am. Chem. Soc.* **1988**, *110*, 1733. (d) Wasielewski, M. R.; Niemczyk, M. P.; Svec, W.; Pewitt, E. B. *J. Am. Chem. Soc.* **1985**, *107*, 5562.
- (3) (a) Jones, W. E., Jr.; Bignozzi, C. A.; Chen, P.; Meyer, T. J. *Inorg. Chem.* **1993**, *32*, 1167. (b) Worl, L. A.; Strouse, G. F.; Younathan, J. N.; Baxter, S. M.; Meyer, T. J. *J. Am. Chem. Soc.* **1990**, *112*, 7571. (c) Meyer, T. J. *Acc. Chem. Res.* **1989**, *22*, 163. (d) Strouse, G. F.; Worl, L. A.; Younathan, J. N.; Meyer, T. J. *J. Am. Chem. Soc.* **1989**, *111*, 9101. (e) Danielson, E.; Elliott, C. M.; Merkert, J. W.; Meyer, T. J. *J. Am. Chem. Soc.* **1987**, *109*, 2519. (f) Olmsted, J., III.; McClanahan, S. F.; Danielson, E.; Younathan, J. N.; Meyer, T. J. *J. Am. Chem. Soc.* **1987**, *109*, 3297. (g) Margerum, L. D.; Murray, R. W.; Meyer, T. J. *J. Phys. Chem.* **1986**, *90*, 728.
- (4) (a) Mecklenburg, S. L.; Peek, B. M.; Erickson, B. W.; Meyer, T. J. *J. Am. Chem. Soc.* **1991**, *113*, 8540. (b) Mecklenburg, S. L.; Peek, B. M.; Schoonover, J. R.; McCafferty, D. G.; Wall, C. G.; Erickson, B. W.; Meyer, T. J. *J. Am. Chem. Soc.* **1993**, *115*, 5479.
- (5) (a) Inai, Y.; Sisido, M.; Imanishi, Y. *J. Phys. Chem.* **1991**, *95*, 3847. (b) Sisido, M.; Tanaka, R.; Inai, Y.; Imanishi, Y. *J. Am. Chem. Soc.* **1989**, *111*, 6790.
- (6) Schanze, K. S.; Sauer, K. J. *J. Am. Chem. Soc.* **1988**, *110*, 1180.

- (7) (a) Vassilian, A.; Wishart, J. F.; van Hemelryck, B.; Schwarz, H.; Isied, S. S. *J. Am. Chem. Soc.* **1990**, *112*, 7278. (b) Isied, S. S.; Vassilian, A.; Magnuson, R. H.; Schwarz, H. A. *J. Am. Chem. Soc.*, **1988**, *107*, 7432.
- (8) Abbreviations: bpy or b = 2,2'-bipyridine; Boc = *tert*-butoxycarbonyl; Lys = L-lysine; m = 4'-methyl-2,2'-bipyridine-4-carbonyl; PTZ = 10*H*-phenothiazine; PTZpn = 3-(10*H*-phenothiazine-10)propanoyl; Anq-OH = 9,10-anthraquinone-2-carboxylic acid; Anq = 9,10-anthraquinone-2-carbonyl.
- (9) (a) Peek, B. M.; Ross, G. T.; Edwards, S. W.; Meyer, G. J.; Meyer, T. J.; Erickson, B. W. *Int. J. Peptide Protein Res.* **1991**, *38*, 114. (b) Peek, B. M.; Ross, G. T.; Edwards, S. W.; Meyer, G. J.; Meyer, T. J.; Erickson, B. W.; *Int. J. Peptide Protein Res.* **1991**, *38*, 114. (c) Peek, B. M. Ph.D. Dissertation, University of North Carolina at Chapel Hill, 1991.
- (10) Godefroi, E. F.; Little, E. L. *J. Org. Chem.* **1956**, *21*, 1163.

Chart 1



**9,10-Dihydro-9,10-dioxoanthracene-2-carboxamidomethane, Anq-NHCH<sub>3</sub>.** Solid anthraquinone-2-carboxylic acid (252 mg, 1.0 mmol), methylamine hydrochloride (68 mg, 1.0 mmol, dried overnight under high vacuum), (1-benzotriazoleoxy)tris(pyrrrolidino)phosphonium hexafluorophosphate (PyBOP, 572 mg, 1.1 mmol), and 1-hydroxybenzotriazole (HOBT, 149 mg, 1.1 mmol) were suspended in DMF (5 mL) containing *N*-methylmorpholine (NMM, 334 mg, 3.3 mmol). The mixture was warmed to 35 °C and stirred for 20 h. The DMF was removed under high vacuum, and the resulting solid was dissolved in ethyl acetate (50 mL), extracted with saturated NaHCO<sub>3</sub> (2 × 50 mL) and brine (2 × 50 mL), and dried with MgSO<sub>4</sub>. Evaporation of solvent left a yellow solid, which was recrystallized from acetone to afford pure Anq-NHCH<sub>3</sub> (145 mg, 55% yield after recrystallization) as fine yellow needles: mp 212.0–214.0 °C; UV (CH<sub>3</sub>CN) λ (ε) 256 (15 100) and 456 nm (2600 L cm<sup>-1</sup> mol<sup>-1</sup>); <sup>1</sup>H NMR (400 MHz, CDCl<sub>3</sub>) δ 3.10 (d, *J* = 4.9 Hz, 3 H, N-CH<sub>3</sub>), 6.59 (br s, 1 H, NH), 7.83–7.85 (dd, *J* = 3.4 Hz, *J* = 3.1 Hz, 2 H, Anq-3,4), 8.30–8.41 (m, 4 H, Anq-5,6,7,8), and 8.57 ppm (d, *J* = 1.8 Hz, 1 H, Anq-1). Anal. Calcd for C<sub>16</sub>H<sub>11</sub>NO<sub>3</sub>: C, 74.45; H, 4.18; N, 5.28. Found: C, 74.33; H, 4.26; N, 5.19.

**N<sup>+</sup>-(1,1-Dimethylethoxycarbonyl)-N<sup>+</sup>-(bis(2,2'-bipyridine)(4'-methyl-2,2'-bipyridine-4-carbonyl)ruthenium(II))-L-lysine Bis(hexafluorophosphate), [Boc-Lys(Rub<sub>2</sub>m)<sup>2+</sup>-OH](PF<sub>6</sub>)<sub>2</sub>.** Lithium hydroxide monohydrate (LiOH, 60 mg, 1.4 mmol) was added to a stirring solution of [Boc-Lys(Rub<sub>2</sub>m)<sup>2+</sup>-OCH<sub>3</sub>](PF<sub>6</sub>)<sub>2</sub><sup>4b</sup> (185 mg, 0.161 mmol) in 3:1 (v/v) methanol–water (5 mL) at room temperature. After 2 h the methanol was removed by rotary evaporation, water (10 mL) was added, and the solution was acidified to pH 2 with 60% HPF<sub>6</sub>. The orange solid that precipitated was collected on a medium-porosity fritted glass filter, washed with diethyl ether (3 × 10 mL), redissolved in acetonitrile (1 mL), and dripped into rapidly stirring ice-cold diethyl ether (200 mL). The bright orange solid that precipitated was collected on a medium-porosity glass frit and vacuum-dried to afford pure [Boc-Lys(Rub<sub>2</sub>m)<sup>2+</sup>-OH](PF<sub>6</sub>)<sub>2</sub> (174 mg, 95% yield): UV (CH<sub>3</sub>CN) λ (ε) 246 (14 800), 288 (37 700), and 456 nm (8800 L cm<sup>-1</sup> mol<sup>-1</sup>); FAB-MS (calcd for C<sub>43</sub>H<sub>46</sub>F<sub>6</sub>N<sub>8</sub>O<sub>5</sub>PRu [(M - PF<sub>6</sub>)<sup>+</sup>], *m/z* 1001.2276) *m/z* 1001.2281; <sup>1</sup>H NMR ((CD<sub>3</sub>)<sub>2</sub>CO) δ 1.37 (s, 9 H, (CH<sub>3</sub>)<sub>3</sub>C), 1.30–1.95 (m, 6 H, γ-CH<sub>2</sub>, β-CH<sub>2</sub>, δ-CH<sub>2</sub>), 2.60 (s, 3 H, m<sup>4</sup>-CH<sub>3</sub>), 3.39–3.46 (m, 2 H, ε-CH<sub>2</sub>), 4.05–4.17 (m, 1 H, α-H), 6.13 (d, *J* = 8.46 Hz, 1 H, N<sup>+</sup>H), 7.45 (d, *J* = 4.9 Hz, 1 H, m<sup>5</sup>), 7.53–7.62 (m, 4 H, b5), 7.86–8.25 (m, 12 H, N<sup>+</sup>H, m5, m6, m6', 4 × (b4, b6)), 8.80 (d, 5 H, m3', 4 × b3), and 9.07 ppm (broad s, 1 H, m3). Anal. Calcd for C<sub>43</sub>H<sub>46</sub>F<sub>12</sub>N<sub>8</sub>O<sub>5</sub>P<sub>2</sub>Ru·(C<sub>2</sub>H<sub>5</sub>)<sub>2</sub>O: C, 46.27; H, 4.63; N, 9.18. Found: C, 46.12; H, 4.43; N, 9.60.

**N<sup>+</sup>-(1,1-Dimethylethoxycarbonyl)-N<sup>+</sup>-(bis(2,2'-bipyridine)(4'-methyl-2,2'-bipyridine-4-carbonyl)ruthenium(II))-L-lysine 3-(10*H*-phenothiazine-10)propylamide Bis(hexafluorophosphate), [Boc-Lys(Rub<sub>2</sub>m)<sup>2+</sup>-NH-prPTZ](PF<sub>6</sub>)<sub>2</sub>.** Light was excluded from this reaction at all times. Solid PTZpr-NH<sub>3</sub>Cl<sup>4b,10</sup> (67 mg, 0.231 mmol), PyBOP (120 mg, 0.231 mmol), and HOBT (33 mg, 0.231 mmol) were added to a solution of [Boc-Lys(Rub<sub>2</sub>m)<sup>2+</sup>-OH](PF<sub>6</sub>)<sub>2</sub> (174 mg, 0.154 mmol) and NMM (0.76 mL, 0.693 mmol) in DMF (2 mL). After the reaction was stirred overnight, the DMF was removed under reduced pressure, and the resulting oil was chromatographed on a neutral alumina column (2.5 cm × 25 cm) by elution with 2:1 CH<sub>3</sub>CN/toluene. Evaporation of solvent afforded pure [Boc-Lys(Rub<sub>2</sub>m)<sup>2+</sup>-NH-prPTZ](PF<sub>6</sub>)<sub>2</sub> (127 mg, 60% yield) as an orange oil: UV (CH<sub>3</sub>CN) λ (ε) 254 (40 600), 288 (55 300), and 456 nm

(11 900 L cm<sup>-1</sup> mol<sup>-1</sup>); FAB-MS (calcd for C<sub>58</sub>H<sub>60</sub>N<sub>10</sub>O<sub>3</sub>RuS [(M - 2PF<sub>6</sub>)<sup>+</sup>], *m/z* 1078.3072) *m/z* 1078.3079; <sup>1</sup>H NMR (250 MHz, CD<sub>2</sub>-Cl<sub>2</sub>) δ 1.34 (s, 9 H, C(CH<sub>3</sub>)<sub>3</sub>), 1.34–1.66 (m, 4 H, β-CH<sub>2</sub>, γ-CH<sub>2</sub>), 1.74–1.99 (m, 4 H, 2-prPTZ, δ-CH<sub>2</sub>), 2.57 (s, 3 H, m-CH<sub>3</sub>), 3.14 (m, 2 H, 1-prPTZ), 3.31–3.36 (m, 2 H, ε-CH<sub>2</sub>), 3.95–4.08 (m, 3 H, 3-prPTZ, α-H), 6.04 (d, *J* = 7.9 Hz, 1 H, α-NH), 6.91–7.29 (m, 9 H, ar PTZ, ε-NH), 7.41 (d, *J* = 5.7 Hz, 1 H, m-5'), 7.52–7.58 (m, 3 H, ar H), 7.85 (d, *J* = 5.7 Hz, 1 H, m5), 8.00–8.22 (m, 10 H, ar H), 8.76–8.80 (m, 6 H, ar H), and 9.05 ppm (s, 1 H, m3). Anal. Calcd for C<sub>58</sub>H<sub>60</sub>F<sub>12</sub>N<sub>10</sub>O<sub>3</sub>P<sub>2</sub>SRu: C, 50.92; H, 4.42; N, 10.24. Found: C, 50.90; H, 4.46; N, 10.21.

**N<sup>+</sup>-(9,10-dihydro-9,10-dioxoanthracene-2-carbonyl)-N<sup>+</sup>-(bis(2,2'-bipyridine)(4'-methyl-2,2'-bipyridine-4-carbonyl)ruthenium(II))-L-lysine Methyl Ester Bis(hexafluorophosphate), [Anq-Lys(Rub<sub>2</sub>m)<sup>2+</sup>-OCH<sub>3</sub>](PF<sub>6</sub>)<sub>2</sub>.** A solution of [Boc-Lys(Rub<sub>2</sub>m)<sup>2+</sup>-OCH<sub>3</sub>](PF<sub>6</sub>)<sub>2</sub> (97 mg, 0.084 mmol) in 4 N HCl/dioxane (10 mL) was stirred at room temperature for 1 h and was then freed of solvent and excess HCl by evaporation under high vacuum (0.2 Torr) for 16 h. The resulting solid amine hydrochloride, [H-Lys(Rub<sub>2</sub>m)<sup>2+</sup>-OMe](PF<sub>6</sub>)<sub>2</sub>(HCl), was suspended in anhydrous DMF (3 mL) and used immediately. Anthraquinone-2-carboxylic acid (Anq-OH, 21 mg, 0.10 mmol), PyBOP (44 mg, 0.10 mmol), and NMM (40 mg, 0.40 mmol) were added, and the DMF suspension was stirred at room temperature for 24 h. The DMF was removed under reduced pressure, and the resulting oil was purified by cation-exchange HPLC to afford analytically pure [Anq-Lys(Rub<sub>2</sub>m)<sup>2+</sup>-OCH<sub>3</sub>](PF<sub>6</sub>)<sub>2</sub> (37 mg, 34% yield): UV (CH<sub>3</sub>CN) λ (ε) 256 (52 400), 288 (55 500), 326 sh (11 700), and 456 nm (11 700 L cm<sup>-1</sup> mol<sup>-1</sup>); FAB-MS (calcd for C<sub>54</sub>H<sub>46</sub>F<sub>12</sub>N<sub>8</sub>O<sub>6</sub>P<sub>2</sub>Ru [M<sup>+</sup>], *m/z* 1294.1867) *m/z* 1294.1835; <sup>1</sup>H NMR (400 MHz, CD<sub>3</sub>CN) δ 1.52 (br s, 2 H, γ-CH<sub>2</sub>), 1.68 (m, 2 H, β-CH<sub>2</sub>), 2.43 (d, *J* = 7.7 Hz, 3 H, m<sup>4</sup>-CH<sub>3</sub>), 2.82 (br s, 2 H, δ-CH<sub>2</sub>), 3.41 (br s, 2 H, ε-CH<sub>2</sub>), 3.67 (s, 3H, m-OCH<sub>3</sub>), 4.56 (m, 1 H, α-H), 7.20 (t, *J* = 5.6 Hz, 1 H, ε-NH), 7.38 (m, 4 H, ar H), 7.54 (d, *J* = 4.1 Hz, 1 H, m<sup>5</sup>), 7.75 (m, 10 H, ar H), 8.06 (m, 7 H, ar H), 8.47 (m, 5 H, ar H), 8.54 (s, 1 H, Anq-1), and 8.76 ppm (d, *J* = 6.2 Hz, 1 H, m3). Anal. Calcd for C<sub>54</sub>H<sub>46</sub>F<sub>12</sub>N<sub>8</sub>O<sub>6</sub>P<sub>2</sub>Ru: C, 50.07; H, 3.58; N, 8.66. Found: C, 49.97; H, 3.63; N, 8.59.

**N<sup>+</sup>-(9,10-dihydro-9,10-dioxoanthracene-2-carbonyl)-N<sup>+</sup>-(bis(2,2'-bipyridine)(4'-methyl-2,2'-bipyridine-4-carbonyl)ruthenium(II))-L-lysine 3-(10*H*-phenothiazine-10)propylamide Bis(hexafluorophosphate), [Anq-Lys(Rub<sub>2</sub>m)<sup>2+</sup>-NH-prPTZ](PF<sub>6</sub>)<sub>2</sub>.** Light was excluded from this reaction at all times. A solution of [Boc-Lys(Rub<sub>2</sub>m)<sup>2+</sup>-NH-prPTZ](PF<sub>6</sub>)<sub>2</sub> (43 mg, 0.031 mmol) in 4 N HCl/dioxane (10 mL) was stirred at room temperature for 1 h and then was freed of solvent and excess HCl by evaporation under high vacuum (0.2 Torr) for 16 h. The resulting amine hydrochloride [H-Lys(Rub<sub>2</sub>m)<sup>2+</sup>-NH-prPTZ](PF<sub>6</sub>)<sub>2</sub>(HCl) (40 mg, 0.031 mmol), which was quantitatively isolated as an orange solid, was immediately dissolved in DMF (1 mL) containing Anq-OH (9.4 mg, 0.037 mmol), PyBOP (19 mg, 0.037 mmol), and NMM (10 mg, 0.099 mmol) and stirred at room temperature for 16 h. The DMF was removed under reduced pressure, and the resulting oil was purified by cation-exchange HPLC to afford [Anq-Lys(Rub<sub>2</sub>m)<sup>2+</sup>-NH-prPTZ](PF<sub>6</sub>)<sub>2</sub> (26 mg, 55% yield) as an orange oil: UV (CH<sub>3</sub>CN) λ (ε) 256 (72 200), 288 (58 700), 326 sh (11 800), and 456 nm (11 700 L cm<sup>-1</sup> mol<sup>-1</sup>); FAB-MS (calcd for C<sub>68</sub>H<sub>58</sub>F<sub>12</sub>N<sub>10</sub>O<sub>5</sub>P<sub>2</sub>RuS [M<sup>+</sup>], *m/z* 1518.3519) *m/z* 1518.3514; <sup>1</sup>H NMR (250 MHz, CD<sub>3</sub>CN) δ 1.25–1.68 (m, 6 H, β-CH<sub>2</sub>, γ-CH<sub>2</sub>,

2 $\delta$ -CH<sub>2</sub>), 1.81–1.89 (m, 2 H, 2-prPTZ), 2.41 (d,  $J = 2.3$  Hz, 3 H, m-CH<sub>3</sub>), 3.24 (t,  $J = 6.8$  Hz, 2 H, 3-prPTZ), 3.40 (m, 2 H, e-CH<sub>2</sub>), 3.85 (t,  $J = 6.8$  Hz, CH<sub>2</sub>-PTZ), 4.40 (m, 1 H,  $\alpha$ -H), 6.84–6.92 (m, 4 H, PTZ), 7.06–7.19 (m, 4 H, PTZ), 7.23–7.41 (m, 4 H, Anq, b<sub>2</sub>m), 7.51 (d,  $J = 5.7$  Hz, m5'), 7.61–7.70 (m, 7 H, Anq, b<sub>2</sub>m), 7.80–8.09 (m, 6 H, Anq, b<sub>2</sub>m), 8.42–8.49 (m, 5 H, Anq, b<sub>2</sub>m), 8.61 (s, 1 H, Anq-1), and 8.84 ppm (d,  $J = 7.9$  Hz, 1 H, m3). Anal. Calcd for C<sub>68</sub>H<sub>58</sub>F<sub>12</sub>N<sub>10</sub>O<sub>5</sub>P<sub>2</sub>SRu: C, 53.79; H, 3.85; N, 9.23. Found: C, 53.72; H, 3.93; N, 9.19.

**Electrochemistry.** Tetrakis(1-butyl)ammonium hexafluorophosphate, [(*n*-C<sub>4</sub>H<sub>9</sub>)<sub>4</sub>N](PF<sub>6</sub>) (Fluka), was twice recrystallized from ethanol and vacuum dried for 10 h. UV-grade CH<sub>3</sub>CN (Burdick and Jackson) was used as received. Each cyclic voltammogram was recorded in a three-compartment cell in a CH<sub>3</sub>CN solution containing 0.1 M [(*n*-C<sub>4</sub>H<sub>9</sub>)<sub>4</sub>N](PF<sub>6</sub>) as the supporting electrolyte. A computer-interfaced Princeton Applied Research Model 273 potentiostat/galvanostat, a silver/silver nitrate (0.1 M) reference electrode, a platinum-wire auxiliary electrode, and a BAS MF-2013 platinum-disk working electrode (0.31 cm<sup>2</sup> electrode area) were used. The scan rate was 100 mV/s, and the measurements were performed inside a dry, N<sub>2</sub>-atmosphere glovebox. Values of  $E_{1/2}$  were calculated by averaging the oxidative ( $E_{p,a}$ ) and reductive ( $E_{p,c}$ ) peak potentials and were not corrected for junction potentials. All values of  $E_{1/2}$  are reported versus the SSCE reference electrode.

**Spectroelectrochemistry.** Absorption spectra of electrochemically reduced species were obtained with an optically transparent thin-layer electrode made of a platinum (90%)–rhodium (10%) grid (Johnson Mathey) placed between the windows of a 2-mm spectrophotometric cell directly mounted in a Hewlett-Packard Model 9451A UV/vis diode-array spectrophotometer. The counter electrode was a Pt wire separated from the cathodic compartment by a glass frit; a Ag wire was the reference electrode. A Princeton Applied Research Model 173 potentiostat/175 universal programmer and a Soltec Model VP6414S chart recorder were used. The spectroelectrochemical experiment was carried out in CH<sub>3</sub>CN (Burdick and Jackson) containing 0.1 M [(*n*-C<sub>4</sub>H<sub>9</sub>)<sub>4</sub>N](PF<sub>6</sub>) (Fluka) as the supporting electrolyte. Before reduction, the solution was purged with dry N<sub>2</sub> for 15 min directly in the spectrophotometric cell. In the controlled-potential electrolysis experiments, the final electronic spectrum of the reduced species was assumed to have been reached when the absorption spectrum no longer changed and when the current was minimal.

A sample of the one-electron reduced species (Anq<sup>•-</sup>)-NHCH<sub>3</sub> was prepared in the N<sub>2</sub>-atmosphere drybox for study by continuous-wave (CW) resonance Raman spectroscopy. Using the three-compartment cell, electrodes, and instrumentation described above for the Electrochemistry section, a cyclic voltammogram of a 4  $\times$  10<sup>-4</sup> M solution of Anq-NHCH<sub>3</sub> in 0.1 M [(*n*-C<sub>4</sub>H<sub>9</sub>)<sub>4</sub>N](PF<sub>6</sub>)/CH<sub>3</sub>CN was obtained (reversible, one-electron reductions were observed at -0.84 and -1.47 V vs SSCE). The Pt disk working electrode was then replaced with a Pt mesh electrode (mesh area  $\sim$ 6 mm  $\times$  20 mm). Constant-potential electrolysis was performed for  $\sim$ 30 min at -1.0 V with continuous stirring. The solution gradually turned a deep purple color. After  $\sim$ 30 min the current passed was reduced to <5% of the maximum. A 1-mL portion of the purple solution was transferred to a 5-mm NMR tube, which was then attached to a tip-off manifold and removed from the drybox. The sample was then freeze-pump-thaw degassed to 10<sup>-6</sup> Torr and sealed. In a similar manner, a sample of 10-(MePTZ<sup>•+</sup>) was prepared. The constant-potential oxidative electrolysis was carried out at +0.8 V vs SSCE for  $\sim$ 5 min. When prepared under these conditions and stored in the dark, the radical ions remains stable for several months.

**Photophysical Measurements.** Luminescence spectra were obtained with a SPEX Fluorolog Model 212 photon-counting spectrofluorimeter with 460-nm excitation and 2-mm slit width and were corrected for the instrument response. Emission quantum yields ( $\Phi_{em}$ ) were measured in optically dilute CH<sub>3</sub>CN solutions ( $A_{460} = 0.09$ – $0.13$ ,  $\sim 1 \times 10^{-5}$  M) relative to [Ru<sup>II</sup>(bpy)<sub>3</sub>](PF<sub>6</sub>)<sub>2</sub> for which  $\Phi_{em} = 0.0615$  in CH<sub>3</sub>CN at 295 K.<sup>11</sup> The quantum yields were calculated as reported previously.<sup>12</sup>

Emission lifetimes and nanosecond transient absorption spectra and kinetics were measured as described previously.<sup>4b</sup> Samples dissolved in UV-grade CH<sub>3</sub>CN (Burdick and Jackson) had an absorbance of 0.1–0.2 at 460 nm ( $\sim (1$ – $2) \times 10^{-5}$  M) in a 1-cm quartz cuvette and were deoxygenated by bubbling with high-purity argon for at least 10 min. For full-spectrum transient absorption measurements, a 35-mL sample was degassed by several freeze-pump-thaw cycles to  $\sim 10^{-6}$  Torr in a tippy cell of our own design.<sup>4b</sup> Transient absorption spectra were corrected for emission by subtracting the emission from the transient signal before the

absorbance changes were calculated<sup>13</sup> according to  $\Delta A = \log(I_0/I)$ , where  $I_0$  is the probe light intensity before the laser pulse and  $I$  is the observed signal after the excitation pulse. Both emission and transient absorption decay traces were fitted to a single-exponential decay as described previously.<sup>12</sup>

The triad was incorporated into a polymethylmethacrylate (PMMA) film. Granular PMMA (0.5 g) was dissolved in warm CHCl<sub>3</sub> (7 mL), part of which (3 mL) was transferred to a 1  $\times$  4 cm mold made of Teflon-coated foil. Approximately 0.2 mg of triad was dissolved in a few drops of CH<sub>3</sub>CN and mixed into the solution in the mold. The solvent was allowed to evaporate from the mold over a period of 3 days. The resulting solid film was placed in a vacuum desiccator for 6 days to remove any remaining solvent from the matrix. The orange, optically transparent, 0.5-mm thick, free-standing film had an absorbance of 0.3 at 420 nm.

Global kinetic analysis of nanosecond transient absorption spectra was performed by using the analysis protocol of Maeder and Zuberbühler.<sup>14a</sup> The program SPECFIT<sup>14b</sup> was modified for kinetic analysis. Factor analysis of the data ( $\Delta A$ ,  $\lambda$ ,  $t$ ) gave a reduced data set, which was fit by a Marquardt nonlinear least-squares algorithm simultaneously at all wavelengths according to a chosen reaction scheme. In the present case, a biexponential function provided an excellent fit to the scheme A  $\rightarrow$  B  $\rightarrow$  C at every wavelength. The spectral components of the transient spectrum in their order of appearance were extracted, and the experimental time evolution of the transient spectrum was reproduced by the data analysis. This procedure provided a very high-quality fit for the nanosecond transient absorption data, with errors for the rate constants in the range 0.3–1.1%.

Continuous-wave resonance Raman spectroscopy was performed at the UNC Laser Laboratory. Laser excitation at 568.2 nm was supplied by a Coherent INNOVA 90K Kr<sup>+</sup> laser. Scattered radiation was collected at 135°, dispersed by an Instruments SA Jobin Yvon (JY) U1000 double monochromator and detected by a thermoelectrically cooled Hamamatsu R943-02 photomultiplier tube. The resulting signal was processed by Instruments SA's Spectra Link photon counting system. Data acquisition was controlled by an IBM PS-2 Model 80 computer with ENHANCED PRISM software from Instruments SA. The sample was contained in a sealed 5-mm NMR tube and spun during excitation.

Transient resonance Raman spectra were obtained<sup>15</sup> by using a 354.7-nm, 4-ns laser pulse to create the excited state and either a 354.7- or a 532-nm pulse as a source for the Raman scattering. The sample was degassed by several freeze-pump-thaw cycles and was sealed in a 5-mm NMR tube. The scattered radiation was collected in a 135° back-scattering geometry into a SPEX Model 1877 Triplemate spectrometer equipped with an 1800 grooves/mm grating. The signal was acquired with a Princeton Instruments Model IRY-700G optical multichannel analyzer (OMA) operated in the gated mode with a Model 110 OSMA detector controller. Timing was controlled by a Princeton Instruments Model FG-100 pulse generator. The final spectrum was the result of a total integration time of 16 min. Laser power was 2.5–3.0 mJ/pulse for each 354.7- and 532-nm laser line. Data collection and storage were controlled by a Gateway 386-MHz computer running the Princeton Instruments SMA software package.

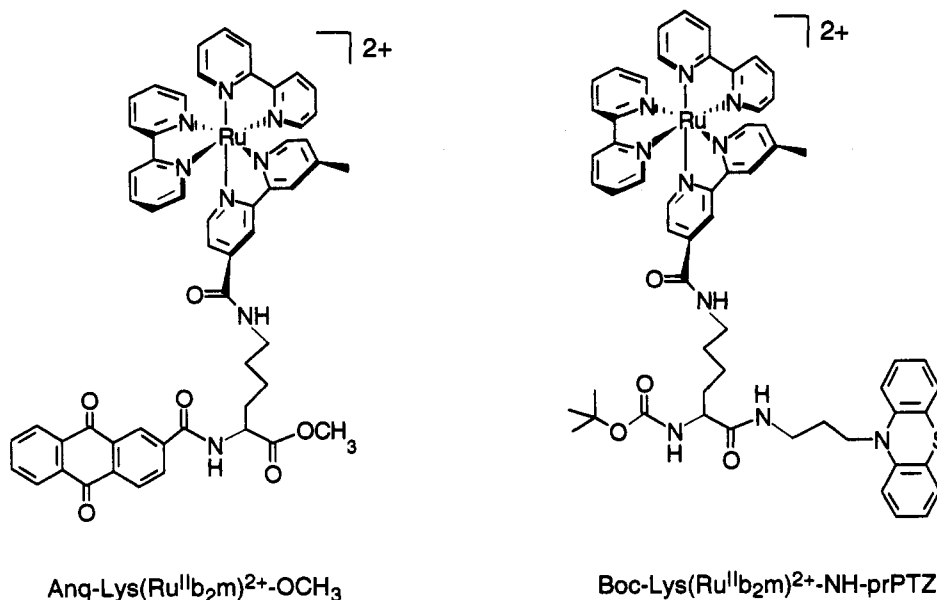
## Results

We continue to apply a modular approach for the assembly of functionalized amino acids that can undergo spatially constrained, photoinduced redox separation.<sup>4</sup> Amino or carboxylic acid derivatives of electron donors, acceptors, and chromophores were prepared and attached to L-lysine through amide bonds. The *tert*-butoxycarbonyl (Boc) protected, chromophoric amino acid [Boc-Lys(Ru<sup>II</sup>b<sub>2</sub>m)<sup>2+</sup>-OH] was condensed with NH<sub>2</sub>-prPTZ to form the model redox dyad [Boc-Lys(Ru<sup>II</sup>b<sub>2</sub>m)<sup>2+</sup>-NH-prPTZ]

(11) Caspar, J. V.; Meyer, T. J. *J. Am. Chem. Soc.* **1983**, *105*, 5583.  
 (12) Chen, P.; Duesing, R.; Graff, D. K.; Meyer, T. J. *J. Phys. Chem.* **1991**, *95*, 5850.

(13) Boyde, S.; Strouse, G. F.; Jones, W. E., Jr.; Meyer, T. J. *J. Am. Chem. Soc.* **1989**, *111*, 7448.  
 (14) (a) Maeder, M.; Zuberbühler, A. D. *Anal. Chem.* **1990**, *62*, 2220. (b) Binstead, R. A.; Zuberbühler, A. D. Global kinetic analysis program SPECFIT, V. 1.0, 1993.  
 (15) (a) Bradley, P. G.; Kress, N.; Hornberger, B. A.; Dallinger, R. F.; Woodruff, W. H. *J. Am. Chem. Soc.* **1981**, *103*, 7441. (b) Mabrouk, P. A.; Wrighton, M. S. *Inorg. Chem.* **1986**, *25*, 526. (c) Strommen, D. P.; Mallick, P. K.; Danzer, G. D.; Lumpkin, R. S.; Kincaid, J. R. *J. Phys. Chem.* **1990**, *94*, 1357. (d) Mallick, P. K.; Strommen, D. P.; Kincaid, J. R. *J. Am. Chem. Soc.* **1990**, *112*, 1686.

Chart 2

Table 1. Photophysical Data in CH<sub>3</sub>CN at 295 K

compd <sup>a</sup>	$\lambda_{MLCT}^b$	$\lambda_{em}^c$	$\Phi_{em}^d$	$\tau_{em},^e$ ns	$\tau_{red},^f$ ns
[Ru <sup>II</sup> (bpy) <sub>3</sub> ] <sup>2+</sup>	452	626	0.062 <sup>g</sup>	920 <sup>h</sup>	
[Ru <sup>II</sup> b <sub>2</sub> m-NHCH <sub>3</sub> ] <sup>2+</sup>	456	645	0.087	1380	
[Anq-Lys(Ru <sup>II</sup> b <sub>2</sub> m) <sup>2+</sup> -OCH <sub>3</sub> ]	456	645	0.002	18	<2
[Boc-Lys(Ru <sup>II</sup> b <sub>2</sub> m) <sup>2+</sup> -NH-prPTZ]	456	645	0.002	15	33
[Anq-Lys(Ru <sup>II</sup> b <sub>2</sub> m) <sup>2+</sup> -NH-prPTZ]	456	645	0.0004	13 <sup>i</sup>	174

<sup>a</sup> All complexes were the PF<sub>6</sub><sup>-</sup> salts. <sup>b</sup> Absorption maximum for MLCT absorption band in nm ( $\pm 2$ ). <sup>c</sup> Emission band maximum in nm ( $\pm 2$ ). <sup>d</sup> Emission quantum yield ( $\pm 10\%$ ). <sup>e</sup> Lifetime ( $\pm 2-4$  ns) obtained by analyzing emission decay curves at the emission maxima following laser excitation at 420 nm. <sup>f</sup> Redox-separated state lifetime ( $\pm 2-4$  ns) obtained by analyzing transient absorption decay curves at 510 and/or 590 nm following laser excitation at 420 nm. <sup>g</sup> Reference 11. <sup>h</sup> Reference 16. <sup>i</sup> The residual emission is attributable to an impurity.

(PF<sub>6</sub>)<sub>2</sub> (Chart 2). Another model dyad [Anq-Lys(Ru<sup>II</sup>b<sub>2</sub>m)<sup>2+</sup>-OCH<sub>3</sub>](PF<sub>6</sub>)<sub>2</sub> was prepared by coupling Anq-OH with the chromophoric amino ester [H<sub>2</sub>N-Lys(Ru<sup>II</sup>b<sub>2</sub>m)<sup>2+</sup>-OCH<sub>3</sub>](PF<sub>6</sub>)<sub>2</sub>.

After deprotection of the amino group of [Boc-Lys(Ru<sup>II</sup>b<sub>2</sub>m)<sup>2+</sup>-NH-prPTZ], an amide bond was formed with the carboxyl group of Anq-OH to give the donor-chromophore-acceptor triad [Anq-Lys(Ru<sup>II</sup>b<sub>2</sub>m)<sup>2+</sup>-NH-prPTZ](PF<sub>6</sub>)<sub>2</sub>. Each compound was purified by cation-exchange HPLC and characterized by fast-atom bombardment (FAB) mass and <sup>1</sup>H NMR spectrometry, UV-vis absorption spectroscopy, cyclic voltammetry, and elemental analysis. The preparation and photophysical properties of the model chromophores [Ru<sup>II</sup>b<sub>2</sub>m-NHCH<sub>3</sub>]<sup>2+</sup>(PF<sub>6</sub>)<sub>2</sub> and [Boc-Lys(Ru<sup>II</sup>b<sub>2</sub>m)<sup>2+</sup>-OCH<sub>3</sub>](PF<sub>6</sub>)<sub>2</sub> have been described in detail.<sup>4,9</sup>

For each complex, a characteristic  $d\pi(Ru^{II}) \rightarrow \pi^*(b,m)$  metal-to-ligand charge-transfer (MLCT) absorption band was observed at 456 nm with  $\epsilon \sim 11\,700$  L mol<sup>-1</sup> cm<sup>-1</sup> (Table 1). The UV-vis absorption spectra of the chromophore [Ru<sup>II</sup>b<sub>2</sub>m-NHCH<sub>3</sub>]<sup>2+</sup> and triad [Anq-Lys(Ru<sup>II</sup>b<sub>2</sub>m)<sup>2+</sup>-NH-prPTZ] are shown in Figure 1. Comparison of the two spectra shows that there is an additional absorption in the triad at 258 nm arising from  $\pi \rightarrow \pi^*$  absorptions of prPTZ and Anq and a shoulder in the 325-nm region due to an  $n \rightarrow \pi^*$  absorption of Anq. The  $d\pi \rightarrow \pi^*$  MLCT absorption at 456 nm is not perturbed in the triad relative to the model chromophore.

Electrochemical data are summarized in Table 2. Data for [Ru<sup>II</sup>(bpy)<sub>3</sub>]<sup>2+</sup> are included for comparison. For [Ru<sup>II</sup>b<sub>2</sub>m-NHCH<sub>3</sub>]<sup>2+</sup>, the Ru<sup>III/II</sup> couple occurs at  $E_{1/2} = 1.27$  V in CH<sub>3</sub>CN (vs SSCE), and for the first ligand-based reduction,  $E_{1/2} =$

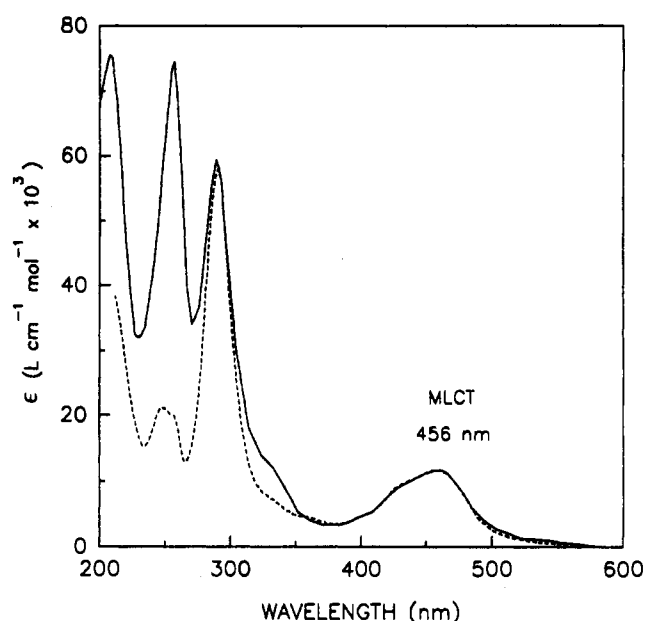


Figure 1. UV-visible absorption spectra for [Ru<sup>II</sup>b<sub>2</sub>m-NHCH<sub>3</sub>]<sup>2+</sup> (---) and [Anq-Lys(Ru<sup>II</sup>b<sub>2</sub>m)<sup>2+</sup>-NH-prPTZ] (—) in CH<sub>3</sub>CN. Samples were  $\sim 5 \times 10^{-4}$  M as the PF<sub>6</sub><sup>-</sup> salts.

Table 2.  $E_{1/2}$  Values in CH<sub>3</sub>CN<sup>a</sup>

compd	prPTZ 0/+	[RuL <sub>3</sub> ]			Anq 0/-
		3+/2+	2+/1+	1+/0	
[Ru <sup>II</sup> (bpy) <sub>3</sub> ] <sup>2+</sup> <sup>b</sup>		1.29	-1.33	-1.52	
[Ru <sup>II</sup> b <sub>2</sub> m-NHCH <sub>3</sub> ] <sup>2+</sup>		1.27	-1.28	-1.51	
[Anq-Lys(Ru <sup>II</sup> b <sub>2</sub> m) <sup>2+</sup> -OCH <sub>3</sub> ]		1.29	-1.25	-1.45	-0.79
[Boc-Lys(Ru <sup>II</sup> b <sub>2</sub> m) <sup>2+</sup> -NH-prPTZ]	0.70 <sup>c</sup>	1.29	-1.25	-1.50	
[Anq-Lys(Ru <sup>II</sup> b <sub>2</sub> m) <sup>2+</sup> -NH-prPTZ]	0.71 <sup>c</sup>	1.31	-1.23	-1.40	-0.83 <sup>d</sup>

<sup>a</sup>  $E_{1/2}$  values ( $\pm 0.02$  V) were obtained in 0.1 M [(*n*-C<sub>4</sub>H<sub>9</sub>)<sub>4</sub>N](PF<sub>6</sub>)/CH<sub>3</sub>CN solutions by taking an average of anodic and cathodic peak potentials in cyclic voltammograms acquired with Pt-disk working, Pt-wire auxiliary, and saturated sodium chloride calomel (SSCE) reference electrodes at a scan rate of 100 mV/s. All compounds were the PF<sub>6</sub><sup>-</sup> salts. <sup>b</sup> Reference 17. <sup>c</sup> Quasi-reversible oxidation. <sup>d</sup> Reduction was irreversible;  $E_{1/2}$  is estimated.

-1.28 V. These potentials are shifted only slightly in the lysine-based assemblies. In addition, the prPTZ<sup>0/+</sup> couple occurs at  $E_{1/2} \sim 0.70$ , and the Anq<sup>0/-</sup> couple occurs at  $E_{1/2} \sim -0.79$  to -0.83 V. An excited-state energy for the chromophore of 2.15 eV was estimated from parameters obtained from emission spectral

(16) Strouse, G. F.; Schoonover, J. R.; Anderson, P. A.; Meyer, T. J.; Keene, F. R. *Inorg. Chem.* 1992, 31, 3004.

(17) Caspar, J. V.; Meyer, T. J. *Inorg. Chem.* 1983, 22, 2444.

fitting of the room-temperature emission spectrum of the model chromophore  $[\text{Ru}^{\text{II}}\text{b}_2\text{m-NHCH}_3]^{2+}$  in  $\text{CH}_3\text{CN}$ , as described previously.<sup>18</sup>

Emission maxima, quantum yields, lifetimes, and redox-separated state lifetimes obtained in  $\text{CH}_3\text{CN}$  are collected in Table 1. Emission from the model chromophore  $[\text{Ru}^{\text{II}}\text{b}_2\text{m-NHCH}_3]^{2+}$  occurred with  $\lambda_{\text{max}} = 645$  nm, a quantum yield of  $0.087 \pm 0.001$ , and a lifetime of 1380 ns in  $\text{CH}_3\text{CN}$ .<sup>4</sup> With an attached electron transfer donor and/or acceptor, the emission was largely quenched. For  $[\text{Boc-Lys}(\text{Ru}^{\text{II}}\text{b}_2\text{m})^{2+}\text{-NH-prPTZ}]$ ,  $\Phi_{\text{em}} = 0.002 \pm 10\%$  and  $\tau_{645} = 14 \pm 4$  ns; for  $[\text{Anq-Lys}(\text{Ru}^{\text{II}}\text{b}_2\text{m})^{2+}\text{-OCH}_3]$ ,  $\Phi_{\text{em}} = 0.002 \pm 10\%$  and  $\tau_{645} = 18 \pm 4$  ns. A weak, residual emission observed from  $[\text{Anq-Lys}(\text{Ru}^{\text{II}}\text{b}_2\text{m})^{2+}\text{-NH-prPTZ}]$ ,  $\Phi_{\text{em}} = 0.0004 \pm 10\%$ ,  $\tau_{645} = 13 \pm 4$  ns, appears to be due to a dyad impurity. These data are summarized in Table 1. Data for the parent complex  $[\text{Ru}^{\text{II}}(\text{bpy})_3]^{2+}$  and for the model chromophore  $[\text{Ru}^{\text{II}}\text{b}_2\text{m-NHCH}_3]^{2+}$  are included for comparison.

Nanosecond transient absorption spectroscopy of the model dyad  $[\text{Anq-Lys}(\text{Ru}^{\text{II}}\text{b}_2\text{m})^{2+}\text{-OCH}_3]$  in argon-bubbled  $\text{CH}_3\text{CN}$  acquired upon 4-ns excitation at 420 nm permitted the observation of rapid quenching of the  $^3\text{MLCT}$  excited state. The 460-nm bleach of the MLCT excited state absorption and the  $\pi \rightarrow \pi^*$  band for the  $\text{m}^{\cdot-}$  radical anion at 370 nm both decayed with a lifetime of 18 ns ( $k = 5.5 \times 10^7 \text{ s}^{-1}$ ). No signals which could be attributed to the Anq $^{\cdot-}$  moiety of the redox-separated state  $[(\text{Anq}^{\cdot-})\text{-Lys}(\text{Ru}^{\text{III}}\text{b}_2\text{m})^{3+}\text{-OCH}_3]$  were observed. In contrast, laser irradiation of the model dyad  $[\text{Boc-Lys}(\text{Ru}^{\text{II}}\text{b}_2\text{m})^{2+}\text{-NH-prPTZ}]$  permitted direct observation of the corresponding redox-separated state  $[\text{Boc-Lys}(\text{Ru}^{\text{II}}\text{b}_2\text{m}^{\cdot+})\text{-NH-(prPTZ}^{\cdot+})]$ , which exhibited transient features at 370 nm ( $\pi \rightarrow \pi^*$ ,  $\text{m}^{\cdot-}$ ) and 510 nm ( $\pi \rightarrow \pi^*$ , prPTZ $^{\cdot+}$ ) that decayed with single-exponential kinetics,  $k = 3.0 \times 10^7 \text{ s}^{-1}$  (33 ns). The bleach at 460 nm recovered with  $k = 7.1 \times 10^7 \text{ s}^{-1}$  (14 ns), and the emission lifetime measured at 645 nm was 15 ns.

Transient absorption difference spectra of the triad  $[\text{Anq-Lys}(\text{Ru}^{\text{II}}\text{b}_2\text{m})^{2+}\text{-NH-prPTZ}]$  in argon-bubbled  $\text{CH}_3\text{CN}$  acquired at various times after excitation with a 420-nm, 4-ns laser pulse ( $\leq 2$  mJ/pulse) are shown in Figure 2. The spectra are corrected for emission as described in the Experimental Section. At 5 ns after the excitation pulse (Figure 2a), increased absorbance at 370 nm due to the substituted bipyridyl anion radical ( $\text{m}^{\cdot-}$ ) and bleaching at 440–460 nm due to the loss of the ground-state,  $\text{d}\pi \rightarrow \pi^*$  (MLCT) transition were observed, in addition to absorptions in the 490–690-nm region. At later times (e.g., 10 ns), the 370-nm absorption decreased, the bleaching disappeared, and absorptions in the visible region increased in intensity with maxima at 510 and 590 nm. The band at 510 nm is due to prPTZ $^{\cdot+}$ ,<sup>19</sup> while the band at 590 nm is due to Anq $^{\cdot-}$ .<sup>20</sup> By 30 ns after the pulse, the difference spectrum corresponded to a superposition of the spectra of prPTZ $^{\cdot+}$  and Anq $^{\cdot-}$ , consistent with the formation of the redox-

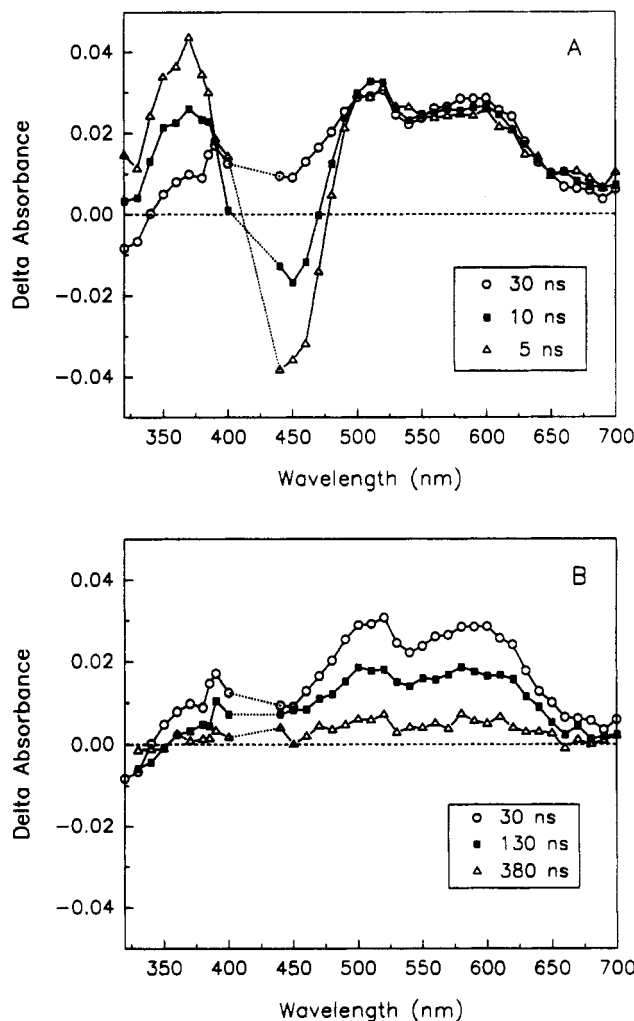


**Figure 2.** Nanosecond transient absorption difference spectra obtained following 420-nm, 4-ns pulsed (1.5 mJ/pulse) excitation of  $[\text{Anq-Lys}(\text{Ru}^{\text{II}}\text{b}_2\text{m})^{2+}\text{-NH-prPTZ}]$  in  $\text{CH}_3\text{CN}$  at 25 °C: Top panel, rise of transient spectrum; bottom panel, decay of transient spectrum.

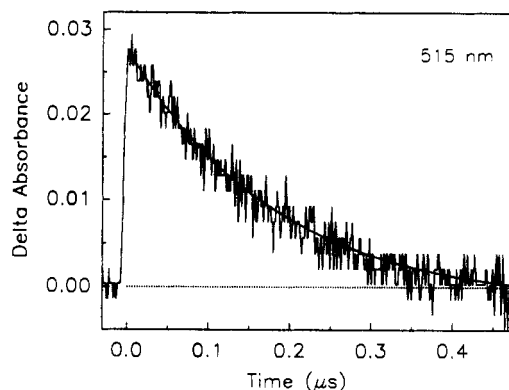


**Figure 3.** Fitted decay trace for data in Figure 2 obtained at 515 nm. The smooth curve is the computer-generated fit to a single exponential function with rate constant of  $k = (5.7 \pm 0.1) \times 10^6 \text{ s}^{-1}$  ( $\tau = 174 \pm 1$  ns).

separated state,  $[(\text{Anq}^{\cdot-})\text{-Lys}(\text{Ru}^{\text{II}}\text{b}_2\text{m})^{2+}\text{-NH-(prPTZ}^{\cdot+})]$  (see Figure 4, discussed below).

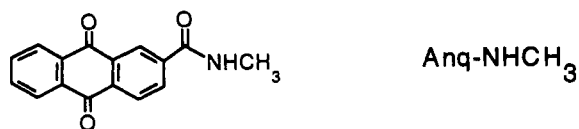
The maximum transient absorbance increase at 590 nm in  $\text{CH}_3\text{CN}$  occurred 30 ns after the excitation pulse, after which the difference spectrum decayed monoexponentially to the baseline with a lifetime of  $174 \pm 3$  ns, as determined by global kinetic analysis.<sup>14</sup> The decay of the spectrum is shown in Figure 2b. An example of a fitted decay trace is shown in Figure 3 for data obtained at 515 nm. The rise and decay of the entire transient absorption data set was rigorously fit by a biexponential function according to the reaction scheme  $\text{A} \rightarrow \text{B} \rightarrow \text{C}$ , where A is the

- (18) (a) Emission spectral fitting was conducted according to established protocols<sup>18b,c</sup> with the use of GOODFIT, a locally written, Simplex-based least-squares fitting program. As described previously,<sup>4b</sup> emission spectral fitting gave values of  $E_0 = 15750 \text{ cm}^{-1}$ ,  $S_M = 1.01$ , and  $\Delta\nu_{0,1/2} = 1870 \text{ cm}^{-1}$ , where  $E_0$  is the difference in energy between the ground and excited states in the  $\nu = 0$  vibrational level of the single, average acceptor vibration,  $S_M$  is the electron-vibrational coupling constant, and  $\Delta\nu_{0,1/2}$  is the full width at half-maximum for the emission band. The excited state energy is given by  $\Delta G_{\text{ex}} = E_0 + \chi_0'$ , where  $\chi_0'$  is the sum of the solvent reorganizational energy and contributions from low-frequency modes treated classically. It is related to the full-width at half-maximum,  $\Delta\nu_{0,1/2}$ , by  $\chi_0' = (\Delta\nu_{0,1/2})^2 / (16k_B T \ln 2)$  which gave  $\chi_0' = 1660 \text{ cm}^{-1}$  at 295 K. (b) Caspar, J. V.; Meyer, T. J. *J. Inorg. Chem.* **1983**, *22*, 2444. (c) Caspar, J. V.; Meyer, T. J. *J. Am. Chem. Soc.* **1983**, *105*, 5583.
- (19) (a) Alkaiatis, S. A.; Beck, G.; Grätzel, M. *J. Am. Chem. Soc.* **1975**, *97*, 5723. (b) Shine, H. J.; Mach, E. E. *J. Org. Chem.* **1965**, *30*, 2130.
- (20) (a) Gamage, R. S. K. A.; McQuillan, A. J.; Peake, B. M. *J. Chem. Soc., Faraday Trans.* **1991**, *87*, 3653. (b) Nakayama, T.; Ushida, K.; Hamanoue, K.; Washio, M.; Tagawa, S.; Tabata, Y. *J. Chem. Soc., Faraday Trans.* **1990**, *86*, 95. (c) Rao, P. S.; Hayon, E. *J. Phys. Chem.* **1973**, *77*, 2274. (d) Fujihira, M.; Hayano, S. *Bul. Chem. Soc. Jpn.* **1972**, *45*, 644. (e) Hulme, B. E.; Phillips, G. O. *J. Chem. Soc., Faraday Trans.* **1972**, *68*, 2003. (f) Fulton, A. *Aust. J. Chem.* **1968**, *21*, 2847.

MLCT excited state, B is the redox-separated state, and C is the final ground state. The first rate constant, quenching of the MLCT excited state and formation of the redox-separated state, was  $8.8 \times 10^7 \text{ s}^{-1}$  (11 ns), while the second rate constant, decay of the redox-separated state, was  $5.7 \times 10^6 \text{ s}^{-1}$  (174 ns). The energy stored in the redox-separated state was 1.54 eV, based on the measured redox potentials of the donor and acceptor of the triad.

The quantum yield for formation of the redox-separated state at its maximum appearance was  $\Phi_{rs} = 0.26 \pm 0.02$  in  $\text{CH}_3\text{CN}$ . The yields of  $\text{Anq}^+$  and  $\text{PTZ}^{2+}$  were measured relative to the known efficiency of cage escape of the paraquat radical cation ( $\text{PQ}^{\bullet+}$ ) following oxidative quenching of the MLCT excited state of  $[\text{Ru}^{\text{II}}(\text{bpy})_3](\text{PF}_6)_2$  by  $\text{PQ}^{2+}$  in  $\text{CH}_3\text{CN}$  after 420-nm excitation.<sup>21</sup> The molar extinction coefficient for  $\text{Anq}^+$  was obtained from the spectroelectrochemical experiment described below. At the  $\lambda_{\text{max}}$  of 592 nm,  $\epsilon = 4000 \pm 100 \text{ L mol}^{-1} \text{ cm}^{-1}$ . A quantum yield of 0.262 was obtained based on the  $\text{Anq}^+$  absorption at 607 nm after correction for absorption of  $\text{PTZ}^{2+}$  at that wavelength. The quantum yield  $\Phi_{rs}$  was also calculated on the basis of the ( $\text{PTZ}^{2+}$ ) transient absorption at 515 nm (corrected for overlap with the  $\text{Anq}^+$  absorption at that wavelength). At 515 nm, based on the literature value for  $\epsilon_{515} = 4560 \text{ M}^{-1} \text{ cm}^{-1}$  for 10-(MePTZ<sup>2+</sup>),<sup>25</sup>  $\Phi_{rs} = 0.255$ . The values of  $\Phi_{rs}$  agree very closely; the experimental error of  $\pm 0.02$  arises from uncertainty in the extinction coefficients of  $\text{Anq}^+$  and  $\text{PTZ}^{2+}$ .

The assignment of the  $\text{Anq}^+$  transient absorption band at 590 nm<sup>20</sup> was confirmed by comparison with the spectrum obtained by a spectroelectrochemical study of  $\text{Anq-NHCH}_3$ . Constant-



potential electrolysis at  $-1.0 \text{ V}$  of a  $5.7 \times 10^{-4} \text{ M}$  sample of  $\text{Anq-NHCH}_3$  in  $0.1 \text{ M } [(n\text{-C}_4\text{H}_9)_4\text{N}](\text{PF}_6)/\text{CH}_3\text{CN}$  gave the spectrum of  $[(\text{Anq}^+)-\text{NHCH}_3]$  shown in Figure 4. Also shown in Figure 4 are the spectrum of 10-MePTZ<sup>2+</sup> and the transient absorption spectrum of the redox-separated state of the triad  $[(\text{Anq}^+)-\text{Lys}(\text{Ru}^{\text{II}}\text{b}_2\text{m})^{2+}\text{-NH-(prPTZ}^{2+})]$  for comparison.

The triad  $[\text{Anq-Lys}(\text{Ru}^{\text{II}}\text{b}_2\text{m})^{2+}\text{-NH-prPTZ}]$  was also studied in 1,2-dichloroethane (DCE; dielectric constant  $\epsilon = 10.4$ ), which is much less polar than  $\text{CH}_3\text{CN}$  ( $\epsilon = 37.5$ ). The emission quantum yield in DCE was  $\Phi_{\text{em}} = 0.04$ , which indicated that the emission of the MLCT excited state was  $\sim 45\%$  quenched. Transient absorption spectroscopy in this solvent determined that the bleaching of the MLCT absorption at 460 nm and the absorption of  $\text{m}^{\bullet-}$  at 370 nm were present with a lifetime  $\tau$  of  $800 \pm 25 \text{ ns}$  ( $k = 1.3 \times 10^6 \text{ s}^{-1}$ ). The emission, monitored at 645 nm, also had a lifetime of  $\tau_{\text{em}} = 800 \pm 25 \text{ ns}$ . Absorptions for the redox-separated state, expected at 510 and 590 nm, were extremely weak with  $\Delta A \sim 0.01$ . The signal-to-noise ratio was too low to determine a lifetime for the redox-separated state in DCE.

$[\text{Anq-Lys}(\text{Ru}^{\text{II}}\text{b}_2\text{m})^{2+}\text{-NH-prPTZ}](\text{PF}_6)_2$  was cast into an optically transparent polymethylmethacrylate (PMMA) film with an absorbance of 0.3 at 420 nm as described in the Experimental Section and was studied by transient absorption spectroscopy. Upon irradiation of the film with a 420-nm, 4-ns pulse, an emission was observed at  $\lambda_{\text{max}} = 600 \text{ nm}$ . The emission decay was not exponential, as observed in previous studies of similar chromophores in PMMA,<sup>22a</sup> but the decay was fit satisfactorily to the Williams-Watts (Kolrausch) function,<sup>22a</sup> eq 1,

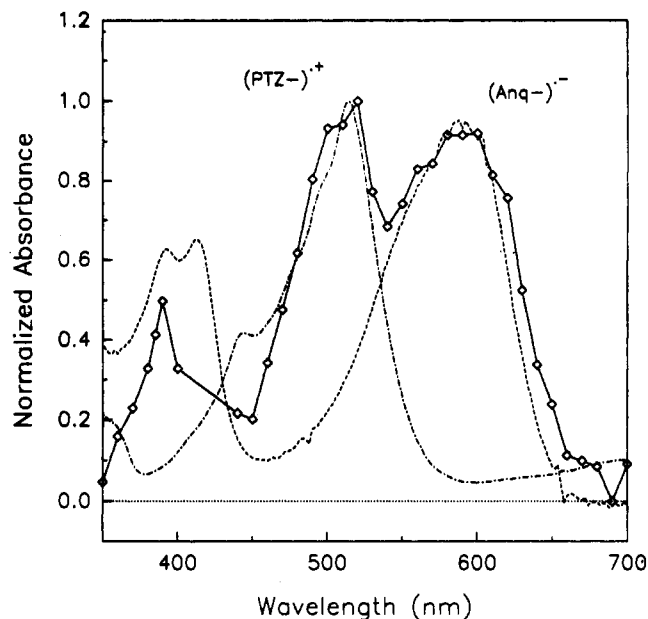


**Figure 4.** Absorption spectrum of  $[(\text{Anq}^+)-\text{NHCH}_3]$  obtained by spectroelectrochemistry upon constant-potential electrolysis at  $-1.0 \text{ V}$  of a  $5.7 \times 10^{-4} \text{ M}$  sample of  $\text{Anq-NHCH}_3$  in  $0.1 \text{ M } [(n\text{-C}_4\text{H}_9)_4\text{N}](\text{PF}_6)/\text{CH}_3\text{CN}$  (---), absorption spectrum of 10-(MePTZ<sup>2+</sup>) in  $0.1 \text{ M } [(n\text{-C}_4\text{H}_9)_4\text{N}](\text{PF}_6)/\text{CH}_3\text{CN}$  obtained similarly by spectroelectrochemistry (—), and transient absorption difference spectrum of  $[(\text{Anq}^+)-\text{Lys}(\text{Ru}^{\text{II}}\text{b}_2\text{m})^{2+}\text{-NH-(prPTZ}^{2+})]$  in  $\text{CH}_3\text{CN}$  obtained at 30 ns after 420-nm, 4-ns excitation ( $\diamond-\diamond$ ). All spectra are normalized for ease of comparison.

**Table 3.** Resonance Raman Frequencies ( $\text{cm}^{-1}$ )<sup>a</sup>

$(\text{Anq}^+)-\text{Lys}(\text{Ru}^{\text{II}}\text{b}_2\text{m})^{2+}\text{-NH-(prPTZ}^{2+})$	$(\text{Anq}^+)-\text{NHCH}_3$	10-MePTZ <sup>2+</sup>
1175	1178	
1294		1291
1333	1340	
1506	1506	
1599		1596

<sup>a</sup> Data were collected as described in the Experimental Section. Frequencies for  $(\text{Anq}^+)-\text{Lys}(\text{Ru}^{\text{II}}\text{b}_2\text{m})^{2+}\text{-NH-(prPTZ}^{2+})$  were obtained by transient resonance Raman spectroscopy in  $\text{CH}_3\text{CN}$ . Frequencies for  $(\text{Anq}^+)-\text{NHCH}_3$  (568.2-nm excitation) and for 10-MePTZ<sup>2+</sup> (514.5-nm excitation) were obtained by CW resonance Raman spectroscopy in  $0.1 \text{ M } [(n\text{-C}_4\text{H}_9)_4\text{N}](\text{PF}_6)/\text{CH}_3\text{CN}$ .

$$I(t) = I_0 e^{-(kt)^\beta} \quad (1)$$

with  $k = 6.25 \times 10^5 \text{ s}^{-1}$ ,  $\beta = 0.81$ , and  $\langle \tau \rangle = 1600 \text{ ns}$ . The MLCT excited state was observed by transient absorption spectroscopy with an absorption at 370 nm ( $\text{m}^{\bullet-}\text{-NHCH}_3$ ) and a bleach at 460 nm (loss of the MLCT absorption). The transients exhibited the same average lifetime as the emission and were also fit to the Williams-Watts function. No transients arising from the redox-separated state of the triad were observed under these conditions.

Time-resolved resonance Raman spectra<sup>15,23</sup> of the model chromophore  $[\text{Ru}^{\text{II}}\text{b}_2\text{m-NHCH}_3]^{2+}$  and the triad  $[\text{Anq-Lys}(\text{Ru}^{\text{II}}\text{b}_2\text{m})^{2+}\text{-NH-prPTZ}]$  in  $\text{CH}_3\text{CN}$  are tabulated in Table 3. Laser pulses at 354.7 and 532 nm were used to excite the sample and as a source for Raman scattering, respectively. In the transient Raman spectrum, bands were observed for  $\text{PTZ}^{2+}$  (1294 and 1599  $\text{cm}^{-1}$ ) and  $\text{Anq}^+$  (1175, 1333, and 1506  $\text{cm}^{-1}$ ), which were consistent with the formation of the redox-separated state. Also listed in Table 3 are bands observed from resonance Raman spectroscopy of  $(\text{Anq}^+)-\text{NHCH}_3$ <sup>24</sup> and 10-(MePTZ<sup>2+</sup>).<sup>25</sup> Bands

(21) Olmsted, J., III.; Meyer, T. J. *J. Phys. Chem.* **1987**, *91*, 1649.  
 (22) (a) Jones, W. E., Jr.; Chen, P.; Meyer, T. J. *J. Am. Chem. Soc.* **1992**, *114*, 387. (b) Chen, P.; Danielson, E.; Meyer, T. J. *J. Phys. Chem.* **1988**, *92*, 3708. (c) Wasielewski, M. R.; Gaines, G. L., III.; O'Neil, M. P.; Niemczyk, M. P.; Svec, W. A. *NATO ASI Ser., Ser. C* **1992**, *371*, 201. (d) Gaines, G. L., III.; O'Neil, M. P.; Svec, W. A.; Niemczyk, M. P.; Wasielewski, M. R. *J. Am. Chem. Soc.* **1991**, *113*, 719.

(23) Schoonover, J. R.; Strouse, G. F.; Chen, P.; Bates, W. D.; Meyer, T. J. *Inorg. Chem.* **1993**, *32*, 2618.

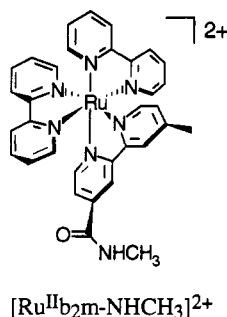
(24) This work. The sample of  $(\text{Anq}^+)-\text{NHCH}_3$  was prepared as described in the Experimental Section.

for bpy<sup>-</sup> (1016, 1035, 1214, 1288, 1429, 1482, and 1550 cm<sup>-1</sup>)<sup>15a</sup> or m<sup>-</sup> (745, 1012, 1037, 1131, 1209, 1283, 1429, 1494, and 1552 cm<sup>-1</sup>)<sup>4b</sup> were not observed in these spectra.

## Discussion

The long-term objective of this work is the development of molecular assemblies containing redox-active modules (electron or energy donors, electron acceptors, and chromophores) that are linked to amino acids through amide bonds.<sup>4,9</sup> These functionalized amino acids can be used to assemble multifunctional peptides having designed structures and specific properties. For example, appropriately structured peptides could undergo spatially controlled, photoinduced electron transfer with redox separation over considerable distances. Also, suitably functionalized peptides could serve as energy-transfer conduits between a light absorber and an emitter. This report describes further progress toward the assembly of such systems. We have expanded the pool of available redox-active modules with the addition of anthraquinone as an electron acceptor. Use of anthraquinone in place of paraquat has several significant advantages. Carboxylic acid derivatives of anthraquinone are commercially available and have a reduction potential ~300 mV more negative than paraquat, which allows more energy to be stored. Finally, anthraquinones are much less toxic than paraquat. The tuning effects of this acceptor on the energy and lifetime of the redox-separated state are described. The redox-separated state [(Anq<sup>-</sup>)-Lys(Ru<sup>II</sup>b<sub>2</sub>m)<sup>2+</sup>-NH-(prPTZ<sup>•+</sup>)] has been observed both by time-resolved resonance Raman spectroscopy<sup>15,16,23</sup> and by nanosecond transient absorption spectroscopy.

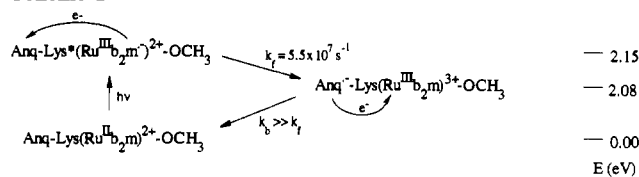
The photophysical properties of the chromophore employed in these assemblies, [Ru<sup>II</sup>b<sub>2</sub>m-NHCH<sub>3</sub>]<sup>2+</sup>, have been described in



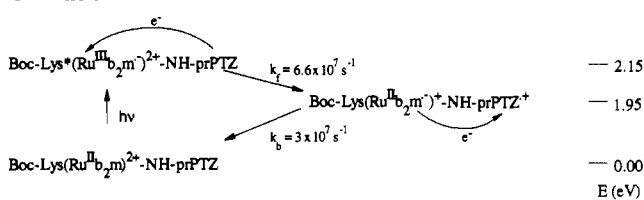
detail.<sup>4b</sup> This mixed chelate has the relatively long <sup>3</sup>MLCT lifetime of 1380 ns in CH<sub>3</sub>CN and is photochemically stable under the conditions used for these studies. It was established previously<sup>4b</sup> by time-resolved resonance Raman spectroscopy that the excited electron resides principally on the m-NHCH<sub>3</sub> ligand, a conclusion consistent with electrochemical measurements (compare the [RuL<sub>3</sub>]<sup>2+/+</sup> couples for [Ru<sup>II</sup>b<sub>2</sub>m-NHCH<sub>3</sub>]<sup>2+</sup> and [Ru<sup>II</sup>(bpy)<sub>3</sub>]<sup>2+</sup> in Table 2). The transient absorption difference spectrum of [Ru<sup>II</sup>b<sub>2</sub>m-NHCH<sub>3</sub>]<sup>2+</sup> is characterized by a strong negative absorption at 460 nm due to bleaching of the MLCT ground-state absorption and a strong positive absorption at 370 nm by the substituted bipyridyl anion radical [(m<sup>-</sup>)-NHCH<sub>3</sub>]. Attachment of [Ru<sup>II</sup>b<sub>2</sub>m]<sup>2+</sup> to the ε-amino group of Boc-L-lysine methyl ester to form Boc-Lys(Ru<sup>II</sup>b<sub>2</sub>m)<sup>2+</sup>-OCH<sub>3</sub>, the scaffold on which more complex redox-active assemblies have been constructed, results in minimal perturbation of these properties.<sup>4b</sup>

**Photophysical Properties of Redox Amino Acids.** In the current work, photoinduced electron transfer was studied in a series of functionalized lysines that incorporated this chromophore. The chromophore-quencher dyads Anq-Lys(Ru<sup>II</sup>b<sub>2</sub>m)<sup>2+</sup>-OCH<sub>3</sub> and Boc-Lys(Ru<sup>II</sup>b<sub>2</sub>m)<sup>2+</sup>-NH-prPTZ were studied as component models for the triad. Upon 420-nm excitation of Anq-Lys-

## Scheme 1



## Scheme 2



(Ru<sup>II</sup>b<sub>2</sub>m)<sup>2+</sup>-OCH<sub>3</sub>, efficient quenching of the MLCT excited state by forward electron transfer from (b<sub>2</sub>m<sup>-</sup>) to Anq occurred with  $k_f = 5.5 \times 10^7 \text{ s}^{-1}$  (18 ns), Scheme 1. The same rate constant was obtained by both emission quenching observed at 645 nm and the decay of the transient absorption for b<sub>2</sub>m<sup>-</sup> at 370 nm. Even though the excited state was efficiently quenched (>97%), Anq<sup>-</sup> could not be detected in the transient absorption experiment, which indicates that decay by back electron transfer from Anq<sup>-</sup> to Ru<sup>III</sup> is sufficiently rapid ( $k > 5 \times 10^8 \text{ s}^{-1}$ ;  $\Delta G^\circ = -2.08 \text{ eV}$ ) that the redox-separated state does not build up in sufficient concentration for observation in the nanosecond experiment.

The chromophore-donor dyad Boc-Lys(Ru<sup>II</sup>b<sub>2</sub>m)<sup>2+</sup>-NH-prPTZ also exhibited efficient quenching of the excited state, but in this case the redox-separated state Boc-Lys[Ru<sup>II</sup>(b<sub>2</sub>m<sup>-</sup>)<sup>+</sup>-NH-(prPTZ<sup>•+</sup>)] was observed in the transient absorption spectrum and decayed with a lifetime of 33 ns, with the absorption by prPTZ<sup>•+</sup> appearing at 510 nm and the absorption by b<sub>2</sub>m<sup>-</sup> at 370 nm. Quenching by forward electron transfer from prPTZ to Ru<sup>III</sup> occurred with  $\Delta G^\circ = -0.20 \text{ eV}$  and  $k = 6.6 \times 10^7 \text{ s}^{-1}$  (15 ns) to form the redox-separated state, which then decays by back electron transfer from b<sub>2</sub>m<sup>-</sup> to prPTZ<sup>•+</sup> with  $\Delta G = -1.95 \text{ eV}$  and  $k = 3 \times 10^7 \text{ s}^{-1}$  (33 ns), Scheme 2.

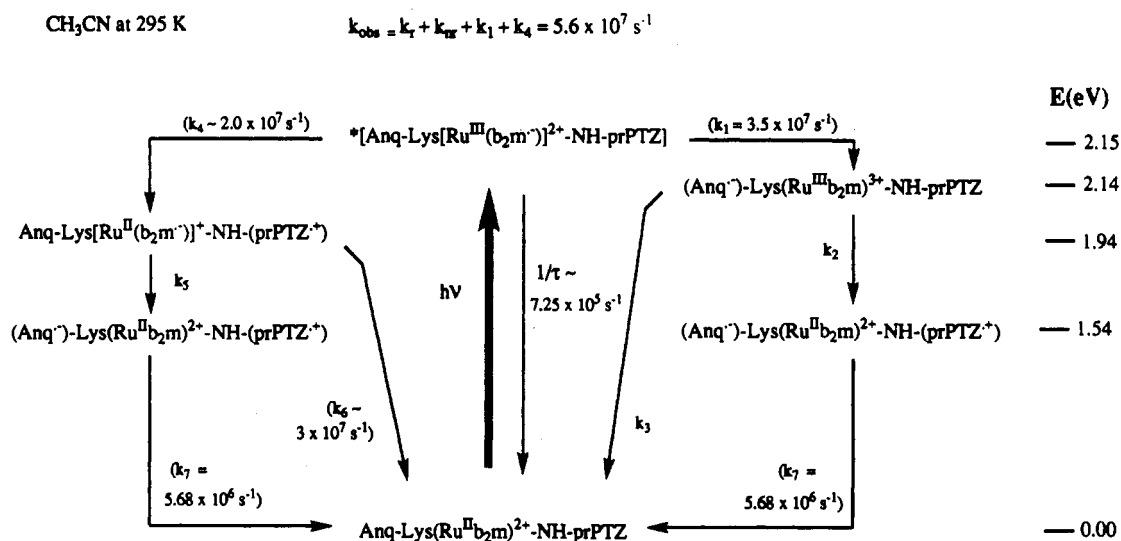
A precedent exists for rapid back electron transfer between oxidative quenchers such as paraquat or diquat and Ru<sup>III</sup>.<sup>26</sup> Previously, we also observed that redox-separated states involving Ru<sup>III</sup> and paraquat radical ions (PQ<sup>•+</sup>) could not be detected even though efficient MLCT quenching occurred.<sup>4b</sup> In contrast, redox-separated states involving PTZ<sup>•+</sup>/m<sup>-</sup> states (such as that in Scheme 2) are readily detected. A contribution to the difference in behavior may come from a difference in energetics. The PTZ<sup>•+</sup>/m<sup>-</sup> state ( $\Delta G^\circ = -2.08 \text{ eV}$ ,  $\lambda = 0.37 \text{ eV}$ ) lies much further into the inverted region and thus decays more slowly than the Ru<sup>III</sup>/PQ<sup>•+</sup> ( $\Delta G^\circ = -1.71 \text{ eV}$ ,  $\lambda = 0.89 \text{ eV}$ ) or Ru<sup>III</sup>/Anq<sup>-</sup> states ( $\Delta G = -2.12 \text{ eV}$ ,  $\lambda = 0.92 \text{ eV}$ ).<sup>27</sup>

(26) (a) Yonemoto, E. H.; Riley, R. L.; Kim, Y. I.; Atherton, S. J.; Schmehl, R. H.; Mallouk, T. E. *J. Am. Chem. Soc.* **1992**, *114*, 8081. (b) Ryu, C. K.; Wang, R.; Schmehl, R. H.; Ferrere, S.; Ludwikow, M.; Merkert, J. W.; Headford, C. E. L.; Elliott, C. M. *J. Am. Chem. Soc.* **1992**, *114*, 430. (c) Schmehl, R. H.; Ryu, C. K.; Elliott, C. M.; Headford, C. E. L.; Ferrere, S. *Adv. Chem. Ser.* **1989**, No. 228, 211. (d) Cooley, L. F.; Headford, C. E. L.; Elliott, C. M.; Kelley, D. F. *J. Am. Chem. Soc.* **1988**, *110*, 6673.

(27) Values of  $\lambda$  were calculated from self-exchange rate constants  $k_{ex}$  as described previously in: Chen, P.; Deusing, R.; Graff, D. K.; Meyer, T. *J. Phys. Chem.* **1991**, *95*, 5850. Calculated values of  $\lambda$  at 298 K and literature references are as follows. (a) bpy<sup>0/-</sup> in CH<sub>3</sub>CN ( $\lambda = 1000 \text{ cm}^{-1}$ ): Reynolds, W. L. *J. Phys. Chem.* **1963**, *67*, 2866. (b) [Ru<sup>II</sup>(bpy)<sub>3</sub>]<sup>3+/2+</sup> in CD<sub>3</sub>CN ( $\lambda = 7300 \text{ cm}^{-1}$ ): Chan, M.-S.; Wahl, A. C. *J. Phys. Chem.* **1978**, *82*, 2542. (c) PTZ<sup>0/+</sup> in CH<sub>3</sub>CN ( $\lambda = 5000 \text{ cm}^{-1}$ ): Kowert, B. A.; Marcoux, L.; Bard, A. J. *J. Am. Chem. Soc.* **1972**, *94*, 5538. (d) Anq<sup>0/-</sup> in CH<sub>3</sub>CN ( $\lambda = 7600 \text{ cm}^{-1}$ ): Meisel, D. E.; Fessenden, R. W. *J. Am. Chem. Soc.* **1976**, *98*, 7505. (e) PQ<sup>2+/+</sup> in CH<sub>3</sub>OH ( $\lambda = 7000 \text{ cm}^{-1}$ ): Dai, S. Ph.D. Dissertation, University of Tennessee, 1990. Private communication from Prof. F. Williams, University of Tennessee.

(25) (a) Hester, R. E.; Williams, K. P. *J. Chem. Soc., Perkin 2* **1981**, 2, 852. (b) This work. The sample of 10-(MePTZ<sup>•+</sup>) was prepared as described in the Experimental Section.

Scheme 3



The triad Anq-Lys(Ru<sup>II</sup>b<sub>2</sub>m)<sup>2+</sup>-NH-prPTZ incorporates an electron donor, a chromophore, and an electron acceptor into the amino acid assembly. Upon excitation of the chromophore, the resulting <sup>3</sup>MLCT state was quenched very efficiently (>99%). An extremely weak, residual luminescence with an emission lifetime of 13 ns was observed from this assembly and is attributed to the presence of a dyad impurity.

Nanosecond, time-resolved absorption spectroscopy of [Anq-Lys(Ru<sup>II</sup>b<sub>2</sub>m)<sup>2+</sup>-NH-prPTZ] provided evidence that the origin of the emission quenching was electron transfer between the excited chromophore and the donor and acceptor, giving rise to the redox-separated state, [(Anq<sup>-</sup>)-Lys(Ru<sup>II</sup>b<sub>2</sub>m)<sup>2+</sup>-NH-(prPTZ<sup>++</sup>)], as outlined in Scheme 3. This state was observed directly by transient absorption spectroscopy through the absorption bands that appeared at 510 nm (prPTZ<sup>++</sup>)<sup>19</sup> and 590 nm (Anq<sup>-</sup>)<sup>20</sup> with  $k_{\text{obs}} = 8.8 \times 10^7 \text{ s}^{-1}$  (11 ns) and decayed with a rate constant of  $k_7 = 5.7 \times 10^6 \text{ s}^{-1}$  (174 ns).

The appearance of the transient spectra of the radical ions Anq<sup>-</sup> and PTZ<sup>++</sup> was confirmed by a spectroelectrochemical study of the models (Anq<sup>-</sup>)-NHCH<sub>3</sub><sup>24</sup> and 10-(MePTZ<sup>++</sup>),<sup>25</sup> as seen in Figure 4. By comparison of these spectra with the transient absorption difference spectrum of the redox-separated state [(Anq<sup>-</sup>)-Lys(Ru<sup>II</sup>b<sub>2</sub>m)<sup>2+</sup>-NH-(prPTZ<sup>++</sup>)], it is clear that the latter spectrum is consistent with a superposition of the absorption features of the radical cation PTZ<sup>++</sup> and the radical anion Anq<sup>-</sup>.

Time-resolved resonance Raman measurements<sup>15,23</sup> further verify the formation of [(Anq<sup>-</sup>)-Lys(Ru<sup>II</sup>b<sub>2</sub>m)<sup>2+</sup>-NH-(prPTZ<sup>++</sup>)] (Table 3). Peaks at 1175, 1333, and 1506 cm<sup>-1</sup> appear due to Anq<sup>-</sup><sup>28</sup> and at 1294 and 1599 cm<sup>-1</sup> due to prPTZ<sup>++</sup>.<sup>25</sup> These assignments were confirmed by comparison with spectra from the literature<sup>25,28</sup> and with the resonance Raman spectra of the radical ions generated electrochemically.

**Kinetic Analysis.** Global kinetic analysis of the entire transient absorption data set was used to obtain the values of  $k_1$  and  $k_7$  as described in the Experimental Section. The transient absorption spectrum was rigorously reproduced by a biexponential function, and an excellent fit to the experimental data was obtained at all wavelengths. The observed monoexponential decay of the redox-separated state implies either that there is a single predominant conformation of the triad in solution or, more likely, that the interconversion between conformers is rapid on the time scale of the electron-transfer events.

A sequence of events that may occur following excitation of the triad is illustrated in Scheme 3. Excitation of the triad produces the <sup>3</sup>MLCT excited state, \*[Anq-Lys(Ru<sup>III</sup>b<sub>2</sub>m)<sup>2+</sup>-NH-prPTZ]. Along the right branch of the scheme, initial

oxidative quenching by Anq ( $k_1$ ) to form [(Anq<sup>-</sup>)-Lys(Ru<sup>III</sup>b<sub>2</sub>m)<sup>3+</sup>-NH-prPTZ] can be followed by either redox-separated state formation ( $k_2$ ) or return to ground state ( $k_3$ ). In the left branch, initial reductive quenching by PTZ ( $k_4$ ) to form [Anq-Lys(Ru<sup>II</sup>b<sub>2</sub>m)<sup>+</sup>-NH-(prPTZ<sup>++</sup>)] can be followed by either redox-separated state formation ( $k_5$ ) or return to ground state ( $k_6$ ). The redox-separated state [(Anq<sup>-</sup>)-Lys(Ru<sup>II</sup>b<sub>2</sub>m)-NH-(prPTZ<sup>++</sup>)] produced from either branch decays back to the ground state by electron transfer from (Anq<sup>-</sup>)- to -(prPTZ<sup>++</sup>) ( $k_7$ ). Estimates for the rate constants in Scheme 3 and their origins are summarized below.

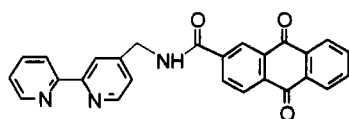
The value for  $k_t + k_{\text{nr}}$  ( $=1/\tau$ ) was taken from the emission lifetime for the model chromophore [Ru<sup>II</sup>b<sub>2</sub>m-NHCH<sub>3</sub>]<sup>2+</sup>, for which  $1/\tau = 7.25 \times 10^5 \text{ s}^{-1}$  in CH<sub>3</sub>CN at 25 °C. The initial quenching step,  $k_{\text{obs}} = 5.6 \times 10^7 \text{ s}^{-1}$  ( $\tau_{\text{obs}} = 11 \text{ ns}$ ), where  $k_{\text{obs}} = k_1 + k_4 + k_t + k_{\text{nr}}$ , was taken from the rate constant for the recovery of the MLCT bleach at 460 nm, which coincided with the rate of appearance of the redox-separated state. The redox-separated state lifetime,  $k_7 = 5.7 \times 10^6 \text{ s}^{-1}$  ( $\tau_7 = 174 \text{ ns}$ ), represents the decay of the transient absorption signals for Anq<sup>-</sup> and prPTZ<sup>++</sup>. Both  $k_{\text{obs}}$  and  $k_7$  were obtained from global analysis of the transient absorption data on the triad.

The appearance of Anq<sup>-</sup> in the redox-separated state of the triad occurs with a rate constant indistinguishable from that for the appearance of prPTZ<sup>++</sup>. This implies that  $k_2$  (and  $k_5$ ) are rapid, on the order of  $>1 \times 10^8 \text{ s}^{-1}$ . A slower rate constant would be detected in this experiment by the observation of an intermediate state resulting from  $k_1$  (or  $k_4$ ) in the global analysis.

The redox-separated state of the PTZ dyad, Boc-Lys-(Ru<sup>II</sup>b<sub>2</sub>m)<sup>2+</sup>-NH-prPTZ, has a lifetime of 33 ns, which provides an estimate for  $k_6 = 3 \times 10^7 \text{ s}^{-1}$  in Scheme 3. There was no evidence for Anq<sup>-</sup> in the transient absorption difference spectrum of the dyad Anq-Lys(Ru<sup>II</sup>b<sub>2</sub>m)<sup>2+</sup>-OCH<sub>3</sub>, even though the MLCT emission was efficiently quenched, from which we expect that  $k_3 \gg k_1$  in Scheme 3 also. We are unable to determine the relative values of  $k_3$  and  $k_2$ , although we estimate that both are likely  $>1 \times 10^8 \text{ s}^{-1}$  on the basis of previous studies<sup>4b</sup> and attempted trapping experiments described below.

The redox-separated state was produced with an efficiency  $\Phi_{\text{rs}} = 0.26 \pm 0.02$  at its maximum appearance at 30 ns following excitation and stored 1.54 eV of energy on the basis of the measured potentials of the donor and acceptor redox couples. From the high degree of emission quenching, initial electron transfer is rapid and efficient. The low efficiency of formation of the redox-separated state must have its origin in the deactivation processes,  $k_3$  and/or  $k_6$  in Scheme 3. On the basis of the behavior of the anthraquinone model dyad, we might make the assumption that decay by  $k_1$  is only followed by  $k_3$  and therefore

no redox-separated state results from initial oxidative quenching. All of the redox-separated state  $[(\text{Anq}^-)\text{-Lys}(\text{Ru}^{\text{II}}\text{b}_2\text{m})^{2+}\text{-NH}(\text{prPTZ}^{*+})]$  would then arise from  $k_4$  followed by  $k_5$ . If we take the direct observations of  $\Phi_{\text{rs}} = 0.26$  and  $k_{\text{obs}} = 5.6 \times 10^7 \text{ s}^{-1}$ , the model chromophore value of  $k_r + k_{\text{nr}} = 7.25 \times 10^5 \text{ s}^{-1}$ , the model dyad value for  $k_6 = 3 \times 10^7 \text{ s}^{-1}$ , and estimate a value for  $k_5 = 1 \times 10^8 \text{ s}^{-1}$ ,  $k_4$  can be calculated from the redox-separated state quantum yield by  $\Phi_{\text{rs}} = (k_4/k_{\text{obs}})[k_5/(k_5 + k_6)]$ . This gives  $k_4 = 2 \times 10^7 \text{ s}^{-1}$ . Use of  $k_{\text{obs}} = k_1 + k_4 + k_r + k_{\text{nr}}$  gives  $k_1 = 4 \times 10^7 \text{ s}^{-1}$ . In this analysis, a major loss of efficiency in redox-separated state formation is in the  $k_1$ - $k_3$  pathway, since if  $k_6$  ( $\sim 3 \times 10^7 \text{ s}^{-1}$ ) is slow relative to  $k_5$  ( $> 1 \times 10^8 \text{ s}^{-1}$ ),  $k_6$  does not contribute significantly to the decay of  $[\text{Anq-Lys}(\text{Ru}^{\text{III}}\text{b}_2\text{m})^{3+}\text{-NH}(\text{prPTZ}^{*+})]$ . Although consistent with the experimental data, the major uncertainty in this analysis is the validity of the assumption that quenching by  $k_1$  does not lead to the redox-separated state. Similar observations have been made in the related complexes  $[\text{Ru}^{\text{II}}(\text{bpy})_2(\text{bpy-AQ})]^{2+}$  and  $[\text{Ru}^{\text{II}}(\text{tmb})_2(\text{bpy-AQ})]^{2+}$  (tmb is 4,4',6,6'-tetramethyl-2,2'-bipyridine; bpy-AQ is shown), in which MLCT quenching is observed but bpy-



bpy-AQ

AQ<sup>-</sup> is not detected. It is not possible to determine whether  $k_2$  is rapid enough to compete with  $k_3$  with our instrumentation. The sequence  $k_1 \rightarrow k_3$  may contribute to redox-separated state formation, but if it is neglected, the analysis gives values for  $k_1$  and  $k_4$  which differ from the quenching rate constants for the model dyads by only a factor of 1.5-3.

This approach to kinetic analysis is supported by the results of a conformational analysis performed previously on the related triad  $[\text{PTZpn-Lys}(\text{Ru}^{\text{II}}\text{b}_2\text{m})^{2+}\text{-NH-prPQ}^{2+}]$ .<sup>4b</sup> In that study it was shown that the lysine-based structure is flexible and various conformations exist that permit close contact between redox-active sites. The advantage of close contact in intramolecular electron transfer, as in outer-sphere electron transfer, is maximizing electronic coupling and minimizing the solvent reorganizational energy.<sup>30</sup> Through-bond electron transfer may also play a role in these systems but probably to a limited degree because of the many saturated bonds that connect the electron-transfer sites. In the PTZ/Rub<sub>2</sub>m<sup>2+</sup>/PQ<sup>2+</sup> triad, energetically favorable conformations are available in which either the donor or the acceptor is situated in a stacked arrangement with one of the chromophore bipyridyl ring systems. We might assume that a similar range of conformational motion is available to the Anq/Rub<sub>2</sub>m<sup>2+</sup>/PTZ triad, noting however that the Anq tether is two instead of four atoms long. If oxidative quenching by Anq ( $k_1$ ) occurs first from a conformation in which Anq is close to the metal center, it is possible that the resulting intermediate would decay rapidly by back-electron-transfer to the nearby Ru<sup>III</sup> ( $k_3$ ) before conformational rearrangement could occur to make secondary reductive quenching by PTZ possible. On the other hand, if PTZ were folded closest to the metal center so that reductive quenching occurred first ( $k_4$ ), it is known from the behavior of the PTZ model dyad that this redox-separated state is able to persist for a significant length of time. Conformational adjustment would permit the second electron transfer to Anq.

**Redox-Separated State Quantum Yield.** The relatively low efficiency of redox-separated state formation ( $\Phi_{\text{rs}} = 0.26 \pm 0.02$  at its maximum appearance) merits more detailed discussion. In the preceding analysis, we attribute the low efficiency of formation

of the redox-separated state to the deactivational process  $k_3$  in Scheme 3 and assume that no redox-separated state results from initial oxidative quenching on the basis of the observed behavior of the model dyad  $[\text{Anq-Lys}(\text{Ru}^{\text{II}}\text{b}_2\text{m})^{2+}\text{-OCH}_3]$ . As stated above, the major uncertainty in this analysis is the validity of the assumption that quenching by  $k_1$  does not lead to the redox-separated state.

In order to further elucidate the  $k_1$ - $k_3$  pathway of Scheme 3, attempts were made to trap the redox-separated state of the model dyad,  $[(\text{Anq}^-)\text{-Lys}(\text{Ru}^{\text{III}}\text{b}_2\text{m})^{3+}\text{-OCH}_3]$ . We have observed that the semiquinone (AQ<sup>-</sup>) can be completely protonated in 1 M trifluoroacetic acid (TFA)/CH<sub>3</sub>CN solutions in  $[\text{Ru}^{\text{II}}(\text{bpy-AQ})_2(\text{bpy-PTZ})]^{2+}$  (see structure of bpy-AQ above) where AQ<sup>-</sup> lives for 150 ns in neat CH<sub>3</sub>CN.<sup>29</sup> Protonation results in complete loss of the AQ<sup>-</sup> absorption band at 590 nm and the appearance of a new band in the 385-nm region for the hydroquinone<sup>20c</sup> (AQH<sup>+</sup>). However, excitation of  $\text{Anq-Lys}(\text{Ru}^{\text{II}}\text{b}_2\text{m})^{2+}\text{-OCH}_3$  in up to 4 M TFA/CH<sub>3</sub>CN has no observable effect on the quenching rate ( $5.6 \times 10^7 \text{ s}^{-1}$ ) and results in no new spectral features. On the basis of this result, the lifetime of  $(\text{Anq}^-)\text{-Lys}(\text{Ru}^{\text{III}}\text{b}_2\text{m})^{3+}\text{-OCH}_3$  must be shorter than  $\sim 250$  ps, thus supporting the hypothesis that  $k_3$  is fast and quenching by  $k_1$  does not lead to the redox-separated state of the triad.

There is no evidence for energy-transfer quenching of the MLCT excited state by Anq- to form the triplet state  $^3(\text{Anq})^*$  in the triad or model dyad. The  $T_1 \rightarrow T_n$  transient absorption spectra of 9,10-anthraquinone and related substituted 9,10-anthraquinones are well-known in the literature.<sup>20b,c,31</sup> For the parent quinone,<sup>20e</sup> the triplet transient absorption maximum appears at 370 nm with  $\epsilon = 10\,200 \text{ M}^{-1} \text{ cm}^{-1}$ . The triplet lifetime is 180 ns in benzene and the triplet energy is 2.72 eV.<sup>20e</sup> Since the MLCT excited state energy of the chromophore is only 2.14 eV, triplet energy transfer is not expected but it would be detected in the transient absorption spectrum of the triad. The  $T_1 \rightarrow T_n$  transient absorption spectrum of the model compound  $\text{Anq-NHCH}_3$  was measured in Ar-bubbled CH<sub>3</sub>CN with 355-nm laser excitation. The absorption maximum appears at 380 nm and the triplet lifetime is  $> 2 \mu\text{s}$ . Since there is no similar species detected in the transient absorption spectra of the triad  $[\text{Anq-Lys}(\text{Ru}^{\text{II}}\text{b}_2\text{m})^{2+}\text{-NH-prPTZ}]$ , energy-transfer quenching is discounted.

**Medium Effects and Energetics.** The study of  $[\text{Anq-Lys}(\text{Ru}^{\text{II}}\text{b}_2\text{m})^{2+}\text{-NH-prPTZ}]$  in a rigid PMMA matrix by transient absorption spectroscopy detected no MLCT quenching upon excitation. This can be understood as a consequence of the rigidity of the surrounding medium. This inhibits the response of the medium to the changes in the local electric field caused by excitation or electron transfer.<sup>22</sup> It has been shown that both oxidative and reductive electron-transfer quenching of rhenium-based MLCT excited states can occur in frozen glasses at 77 K<sup>22b</sup> or in PMMA at room temperature<sup>22a</sup> but only if the driving force for forward electron transfer is sufficiently large (e.g.,  $> 0.5$  eV). In the case of the  $\text{Anq/Rub}_2\text{m}^{2+}/\text{PTZ}$  triad, the forward electron transfer steps have driving forces of 0.21 eV or less. It is therefore not surprising that electron-transfer quenching does not occur in PMMA.

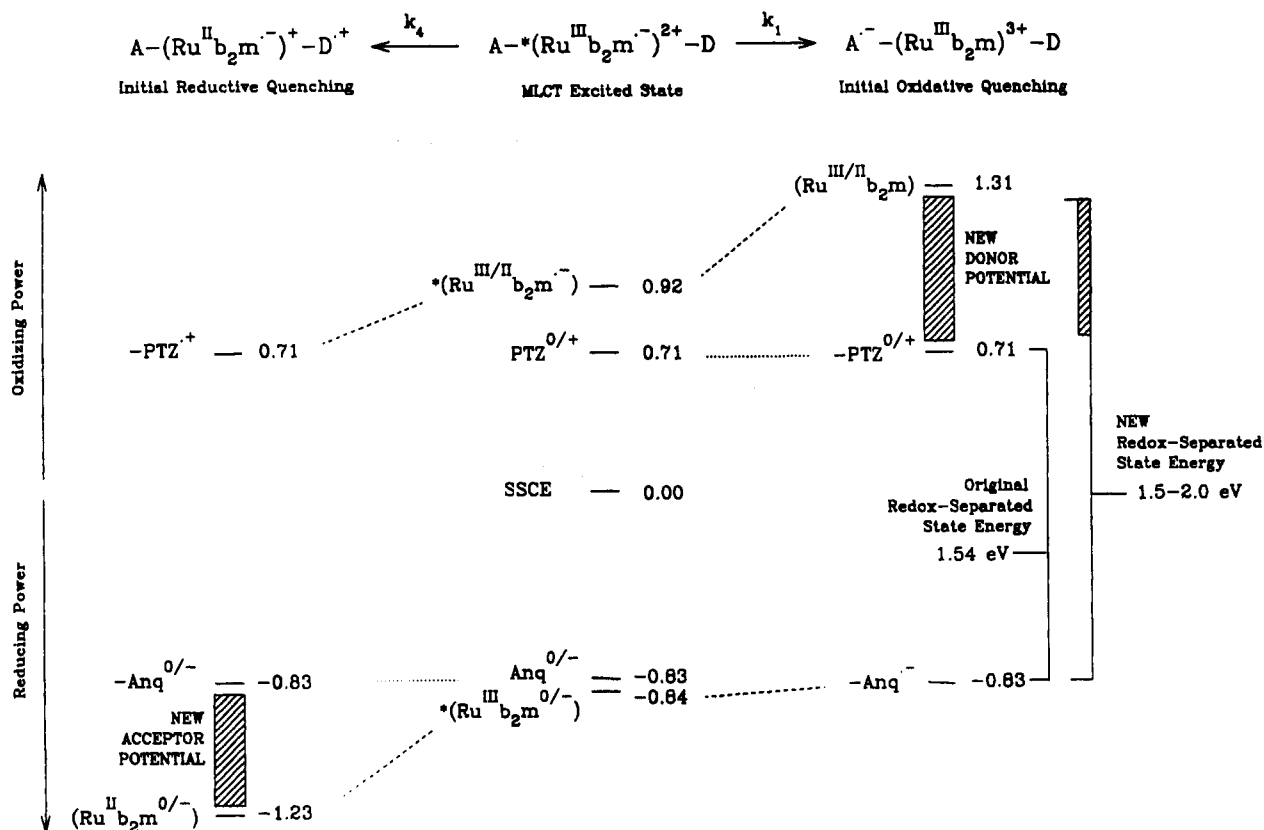
The close energy balance in this system also explains why electron-transfer quenching of the  $^3\text{MLCT}$  excited state is decreased by 2 orders of magnitude in DCE, which is much less polar ( $\epsilon = 10.4$ ) than CH<sub>3</sub>CN ( $\epsilon = 37.5$ ). The amount of redox-separated state observed in DCE was too small for its lifetime to be determined accurately. The emission that was observed was shifted to 621 nm. The emission of the parent chromophore,  $(\text{Ru}^{\text{II}}\text{b}_2\text{m-NHCH}_3)^{2+}$ , occurs at 645 nm in CH<sub>3</sub>CN and at 628 nm in DCE, a shift of 420 cm<sup>-1</sup>. The excited-state energy is

(29) Opperman, K. A.; Mecklenburg, S. L.; Meyer, T. J. *Inorg. Chem.*, submitted for publication.

(30) (a) Sutin, N. *Prog. Inorg. Chem.* **1983**, *30*, 441. (b) Marcus, R. A.; Sutin, N. *Biochim. Biophys. Acta* **1985**, *811*, 265.

(31) (a) Loeff, I.; Treinin, A.; Linschitz, H. *J. Phys. Chem.* **1983**, *87*, 2536. (b) Hamanoue, K.; Kajiwara, Y.; Miyake, T.; Nakayama, T.; Hirase, S.; Teranishi, H. *Chem. Phys. Lett.* **1983**, *94*, 276. (c) Harriman, A.; Mills, A. *Photochem. Photobiol.* **1981**, *33*, 619.

Scheme 4



increased in the less polar solvent as expected, but the energies of the initial states resulting from  $k_1$  and  $k_4$  (in Scheme 3) are increased even more because the electron transfers to the appended quenchers occur over a greater distance than the metal-to-ligand electron transfer that produces the excited state.<sup>32</sup> This increases the energies of these states relative to the MLCT state making intramolecular electron transfer nonspontaneous.

The redox-separated state of the new triad [Anq-Lys-(Ru<sup>II</sup>b<sub>2</sub>m)<sup>2+</sup>-NH-prPTZ] ( $\Delta G^\circ = -1.54$  eV,  $\lambda = 0.78$  eV) stored 0.42 eV more energy than the redox-separated state of the related triad [PTZpn-Lys(Ru<sup>II</sup>b<sub>2</sub>m)<sup>2+</sup>-NH-prPQ<sup>2+</sup>] ( $\Delta G^\circ = -1.17$  eV,  $\lambda = 0.74$  eV), and the resulting state was longer lived, 174 ns vs 108 ns, but at the cost of a somewhat decreased maximum quantum yield, 0.26 (at 30 ns) vs 0.34 (at 35 ns, each  $\pm 8\%$ ). The increase in the redox-separated state lifetime may be attributable to an inverted region effect in which the Anq<sup>-</sup>/PTZ<sup>2+</sup> state ( $|\Delta G^\circ + \lambda| = 0.76$  eV) lies further into the inverted region and thus decays more slowly than the PTZ<sup>2+</sup>/PQ<sup>2+</sup> state ( $\Delta G + \lambda = 0.43$  eV).<sup>27</sup>

(32) (a) According to classical dielectric continuum theory, the difference in energy of interaction with the solvent between two excited states in the same molecule,  $\Delta(\Delta E_s)$ , is given by<sup>31b-f</sup>

$$\Delta(\Delta E_s) = \frac{1}{a^3} (\bar{\mu}_{e,2}^2 - \bar{\mu}_{e,1}^2) \frac{1 - D_1}{2D_1 - 1}$$

where it is assumed that the change in electronic distribution between states can be approximated by a dipole in a sphere of radius  $a$  in a medium of static dielectric constant  $D_s$ , and the quantities  $\bar{\mu}_{e,1}$  and  $\bar{\mu}_{e,2}$  are the dipole moments of excited states 1 and 2. From this equation, it can be inferred that state with the greater electronic displacement (i.e., the states resulting from  $k_1$  and  $k_4$  in Scheme 3) will be destabilized more as the dielectric constant of the solvent is decreased. (b) Tapolski, G.; Duesing, R.; Meyer, T. *J. Phys. Chem.* **1991**, *95*, 1105. (c) Marcus, R. A. *J. Chem. Phys.* **1956**, *24*, 979. (d) Cannon, R. P. *Adv. Inorg. Chem. Radiochem.* **1978**, *21*, 179. (e) Brunshwig, B. S.; Ehrenson, S.; Sutin, N. *J. Phys. Chem.* **1987**, *91*, 4717. (f) Brunshwig, B. S.; Ehrenson, S.; Sutin, N. *J. Phys. Chem.* **1986**, *90*, 3657.

The increase in energy stored by the new system reflects the higher reduction potential of Anq relative to PQ<sup>2+</sup>. In the new system the two redox-quenching steps are poised near the minimum free energy required for either initial quenching event to occur; for  $k_1$ ,  $\Delta G^\circ \sim 0$  eV. For  $k_4$ ,  $\Delta G^\circ = -0.2$  eV. A question of interest is the design of chromophore-quencher combinations that store as much of the excited-state energy as possible. To accomplish this, the quencher redox couples can be varied in one of two ways as illustrated in Scheme 4. The first approach (left and center columns of Scheme 4) is to utilize the donor PTZ and the electron-transfer pathway  $k_4$  of Scheme 3 but to decrease the potential of the acceptor couple to just above the potential of the [Ru<sup>II</sup>b<sub>2</sub>(m<sup>0/-</sup>)]<sup>2+/+</sup> couple at -1.23 V. Reductive electron transfer to PTZ would occur first; then the [Ru<sup>II</sup>b<sub>2</sub>(m<sup>0/-</sup>)]<sup>2+/+</sup> couple is sufficiently reducing to donate an electron to an acceptor at -1.0 to -1.25 V. This would result in the storage of up to  $\sim 2.0$  eV in the resulting redox-separated state. There is a kinetic limit. As  $\Delta G^\circ$  for quenching approaches 0 eV, reversal of the electron-transfer chains and re-formation and decay of the initial MLCT state becomes a pathway for decay of the redox-separated state.

A parallel approach, illustrated in the center and right columns of Scheme 4, is to utilize the acceptor Anq and the  $k_1$  pathway and increase the potential of the donor couple to just below the [(Ru<sup>III/II</sup>)b<sub>2</sub>m]<sup>3+/2+</sup> couple at 1.31 V. On the basis of the results of this analysis and with careful tailoring of the redox energetics, it may prove possible to use this approach to design assemblies where a maximum amount of energy is stored with high efficiency.

**Acknowledgment** is made to the National Science Foundation (Grant CHE-8806664), the National Institute of General Medical Sciences (Grants GM32296 and GM42031), and the North Carolina Biotechnology Center (Grant 8913-ARIG-0104) for support of this research. This investigation was also supported by the National Institute of General Medical Sciences through a National Research Service Award (GM14511) to S.L.M.